PROJECT FIRE MODEL

Summary Progress Report - II

Period May 1, 1960, to April 30, 1962

by

W. L. Fons
H. B. Clements
E. R. Elliott
P. M. George

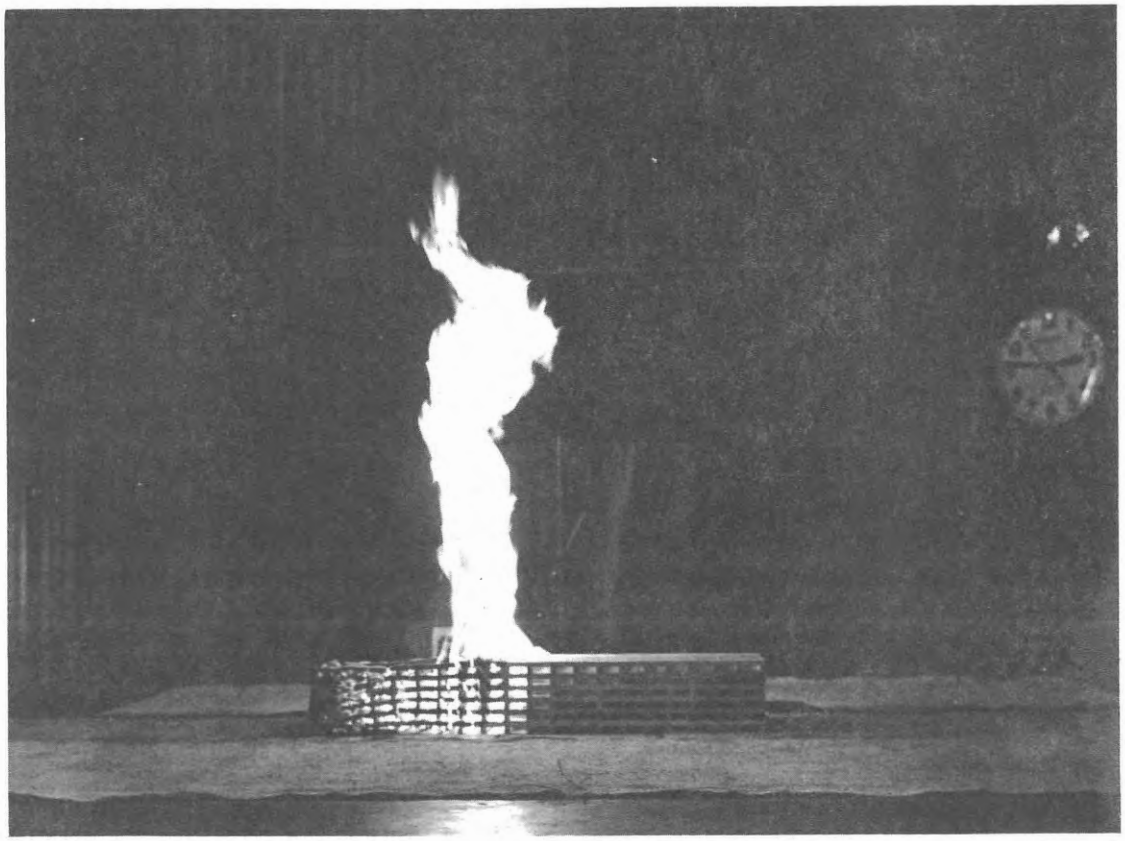

Forest Service, U. S. Department of Agriculture
Southeastern Forest Experiment Station
Southern Forest Fire Laboratory
Macon, Georgia

ACKNOWLEDGMENT

The authors express their thanks to the Office of Civil Defense for providing financial support through contracts administered by the National Bureau of Standards and to the Forest Research Council of the State of Georgia for making facilities available. Credit for assisting in the experimental work, data reduction and calculations is due to R. K. Burgess and M. E. Bishop, of the Southern Forest Fire Laboratory. Finally, the authors express their thanks to H. D. Bruce, W. Y. Pong, and S. S. Richards, of the Pacific Southwest Forest and Range Experiment Station, for their contributions in the initial experimental work.

Material in several sections of this report was presented by W. L. Fons in a paper entitled "Use of Models to Study Forest Fire Behavior" at the Tenth Pacific Science Congress of the Pacific Science Association, held at the University of Hawaii, Honolulu, August 21 to September 6, 1961. The congress was sponsored by the National Academy of Sciences, Bernice Pauahi Bishop Museum, and the University of Hawaii.

CONTENTS

PROJECT FIRE MODEL[1/]

Summary Progress Report - II

Period May 1, 1960 to April 30, 1962

by

W. L. Fons
H. B. Clements
E. R. Elliott
P. M. George

Southern Forest Fire Laboratory
Southeastern Forest Experiment Station
Forest Service, U.S.D.A.

INTRODUCTION

The general objectives of this project are to evaluate the effects of the independent variables of fuel, fuel bed, fuel base, and atmospheric conditions on the dependent variables such as rate of burning, flame size, rate of energy released, and others which are concerned with the spread and control of fires burning in solid fuel. Detailed objectives, scope, and importance of the project and a work plan are presented in an earlier report (Fons et al., 1960). The immediate aim of the project is to explain by means of reliable data the behavior of a laboratory-scale fire burning solid fuels in an unconfined atmosphere. No attempt is made in this report to establish quantitative relations between laboratory-scale and full-scale building or forest fires.

1/ This research was originally sponsored by the Office of Civil and Defense Mobilization (OCDM Contract DCM-SR-59-10) and since April 1960 continued under contract with the National Bureau of Standards (NBS Order No. 35372-60, April 14, 1960, as amended, and NBS Order No. S-302190-62, February 28, 1962).

The propagating flame model selected for study permits establishment of a steady-state condition (Fons et al., 1959) for the free-burning of solid fuels. With this model the parameters which govern combustion can be examined and measured over an extended period of time. The model represents on a reduced scale a section of the combustion zone of a moving fire front burning in a homogeneous fuel bed without spotting.

To date about 100 experimental fires have been burned using this steady-state model. Measurements of the dependent and independent variables were analyzed to establish quantitative relationships between certain fire properties and the fuel and fuel bed parameters. For example, a functional relationship between flame dimensions and the rate of burning was verified. Also, a correlation was found between dimensionless groups containing burning time, flame length, and those parameters which describe the physical properties and the geometry of the fuel and the fuel bed.

EXPERIMENTAL CONDITIONS

The essential elements of the fire model are: a wood fuel bed built in the form of a crib, a combustion table equipped to transport the fuel bed at a controlled rate, an ignition device, a base of inert material of known density, and sensing and recording instruments to measure specific variables (Fons et al., 1959).

The fuel bed is a crib of wood sticks of square cross section. The physical features of such a fuel bed can be controlled. For example, the species, density, moisture content, size and spacing of the wood sticks, and the width and height of the fuel bed are all selected before the crib is built. The crib is formed by placing the sticks in tiers with the selected spacing between sticks. A drop of resorcinol-formaldehyde resin glue is placed on each junction to bond the crib into a rigid assembly. For several weeks before burning, the crib is conditioned to an equilibrium moisture content in an atmosphere of constant temperature and relative humidity.

The ignition device is a narrow, shallow trough containing an asbestos wick saturated with a liquid hydrocarbon. This device is placed at one end of the crib. The liquid hydrocarbon is ignited to initiate combustion in the fuel bed. The fire gradually spreads to the other end of the crib, reducing the wood to a residue of ash and charcoal.

The combustion table is equipped with a chain-belt mechanism which moves the crib and two heavy asbestos sheets, one on each side of the fire, in synchronism with the flame spread to simulate movement of the fire front relative to the ground. The crib and its inert base rest on the chain-belt, which is moved manually by a gear drive in order to hold the flaming zone of the burning crib in a fixed position.

The combustion gases diluted by the entrained air are expelled from the room through a 2-foot-diameter exhaust stack. The incoming

conditioned air is supplied to the room at a rate of about 5,000 cubic feet per minute through several louvered outlets in a continuous duct located near the ceiling around the room. The entrance to the stack is a hood 12 feet in diameter and located 12 feet above the combustion table.

Time-lapse cameras mounted on the wall photograph the test fires for subsequent measurements of flame depth and length. Three grids of thermocouples suspended at different levels above the combustion table measure temperatures of the convection column. A thermocouple and a Pitot tube mounted in the exhaust stack measure the temperature and velocity of combustion gases. Thermopile radiometers located at the front, rear, and side of the test fire measure radiation. The sensing elements are connected to recording instruments in a control room adjacent to the combustion room.

Two important features of the model are: (1) The crib is made relatively long and a zone of fire travels the length of the crib. After an initial buildup, the rate of burning or spread reaches a constant value, which holds until near the end, and thus the difficulty of investigating a fire burning under transient conditions is avoided. (2) The position of the flaming zone is held fixed in space by moving the fuel into the fire. This method permits the grids of thermocouples in the flame and convection column, radiometers surrounding the fire, and other sensing devices to be stationary. The rate of fire spread is equal to the rate the crib is moved to maintain the flame in a fixed position (fig. 1).

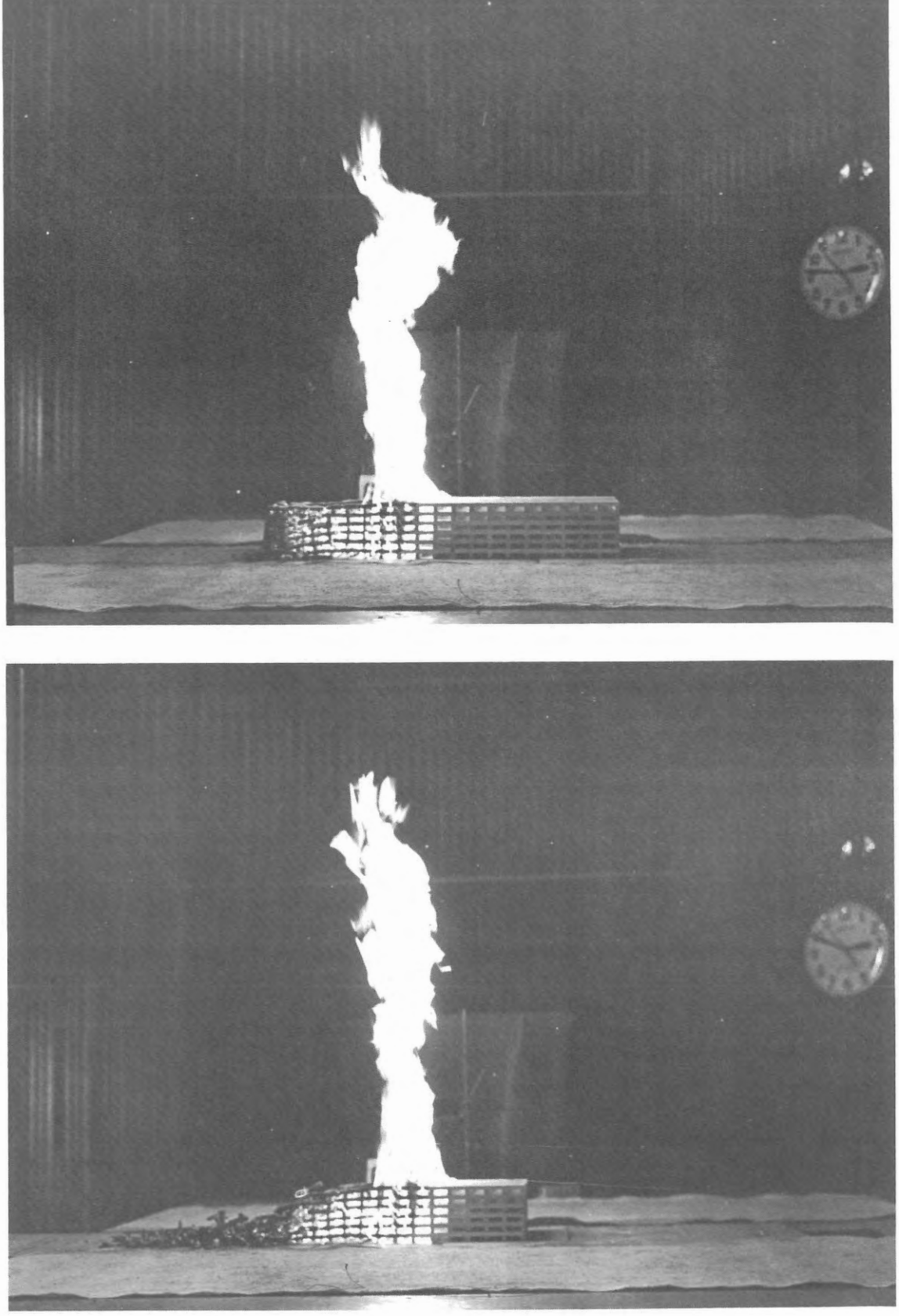

Figure 1. --A test fire at two different times, illustrating the fixed position of the flame as the crib moves.

Physical characteristics of the wood, the crib, and the environment during the burning period for each crib fire are presented in Appendix A, tables 4 and 5. The room temperatures in these tables are the arithmetic means of readings taken before and after each test fire.

The duration of the steady-state burning period is limited only by the buildup time and the length of the crib. The time for the burning to reach a steady-state condition after one end of the crib is ignited depends upon such factors as spacing, density, size and moisture content of the wood sticks. Figure 2 presents curves showing the steady-state periods for the spread of fire through cribs of wood with different specific gravities.

RESULTS AND DISCUSSION

Analyses were made of data from the crib fires to determine quantitative relationships between the several aspects of fire behavior, such as radiative and convective heat, flame dimensions, emissivity, and rate of spread. The experimental data used in the analyses are presented in Appendix A.

1. Heat Value of Wood

Samples of each species of wood covering the full range of densities were reduced to sawdust, molded into pellets, and dried in a desiccator over calcium chloride. The heat values for these samples were determined by an Emerson, adiabatic-type, bomb calorimeter. The high heat values (with moisture condensed to liquid) are presented in table 1.

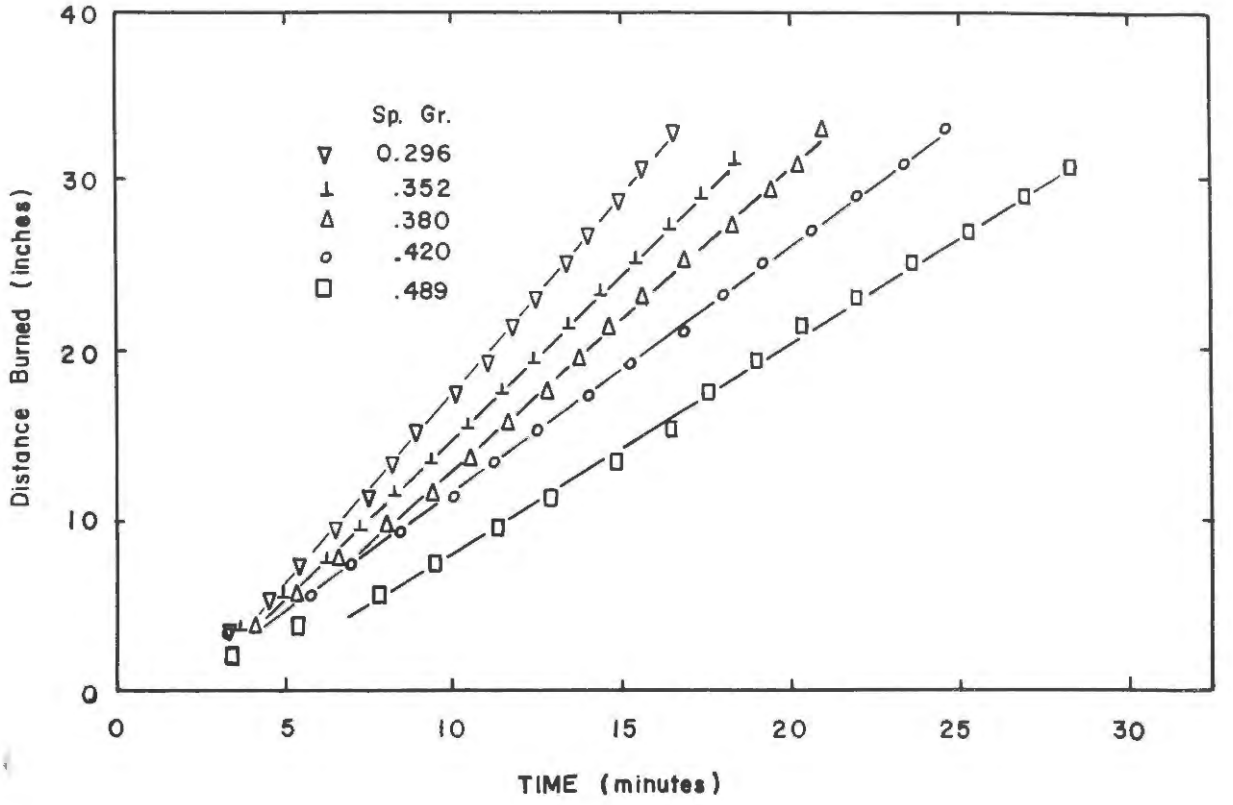

Figure 2. --Steady-state burning through cribs of white fir wood with different specific gravities.

Table 1.--Heat values[1/] for several species of wood

Sample No.	White fir (Abies concolor)	Basswood (Tilia americana)	Magnolia (Magnolia grandiflora)	Sugar maple (Acer saccharum)	Longleaf pine (Pinus palustris)
			HIGH HEAT VALUE, Btu/lb		
1	8576	8408	8614	8573	8801
2	8689	8319	8553	8524	8743
3	8494	8341	8522	8469	8741
4	8748	8321	8606	8599	8826
5	8708	8335	8542	8483	8742
6	8668	8320	8528	8575	--
7	8668	--	--	8579	--
8	8635	--	--	--	--
9	8698	--	--	--	--
10	8702	--	--	--	--
Average	8659	8341	8561	8543	8771
			LOW HEAT VALUE, Btu/lb		
Average	8135	7817	8037	8019	8248

1/ Corrected for moisture content to bone-dry conditions.

In the test fires, the moisture from the fuel does not condense as it does in the bomb calorimeter. Therefore, the low heat value (with moisture in vapor form) is of greater interest than the high heat value. From the measured high heat value of the wood, the low heat value was calculated by assuming that wood is 50 percent carbon, 44 percent oxygen, and 6 percent hydrogen, and on burning forms 0.539 lb. of water vapor for each pound of dry wood. The water vapor, due to its latent heat of vaporization, reduces the high heat value by 0.539 x 972, or 524 Btu/lb. The low heat values for each species of wood, found by subtracting 524 Btu/lb from the high heat values, are also tabulated at the bottom of table 1.

2. Equilibrium Moisture Content of White Fir Wood

The selection and control of the relative humidity of the air supplied to the combustion room were essential in assuring that the moisture content of cribs remains constant during experimental fires. The relative humidity for a given test fire was selected from an equilibrium moisture content curve for wood. For this purpose, an equilibrium moisture content curve was established for white fir wood (fig. 3).

The points on the curve represent the equilibrium moisture content of 25 white fir dowels, 3/8-inch diameter and 9 inches long. The dowels were exposed to selected relative humidities at room temperature 70° F. The relative humidities were produced by saturated salt solutions placed in desiccators. After the dowels had been exposed to the conditions in the desiccators for a period of five months, they were weighed to determine their equilibrium

moisture content. The dry weights of the dowels were determined by Xylene reflux distillation method (Buck and Hughes, 1939). Wood, which tends to be highly hydrated, exhibits different apparent equilibrium values depending on the side from which it is approached. It is believed that the exposure time was sufficiently long to stabilize the values regardless of approach, thus eliminating any hysteresis effect.

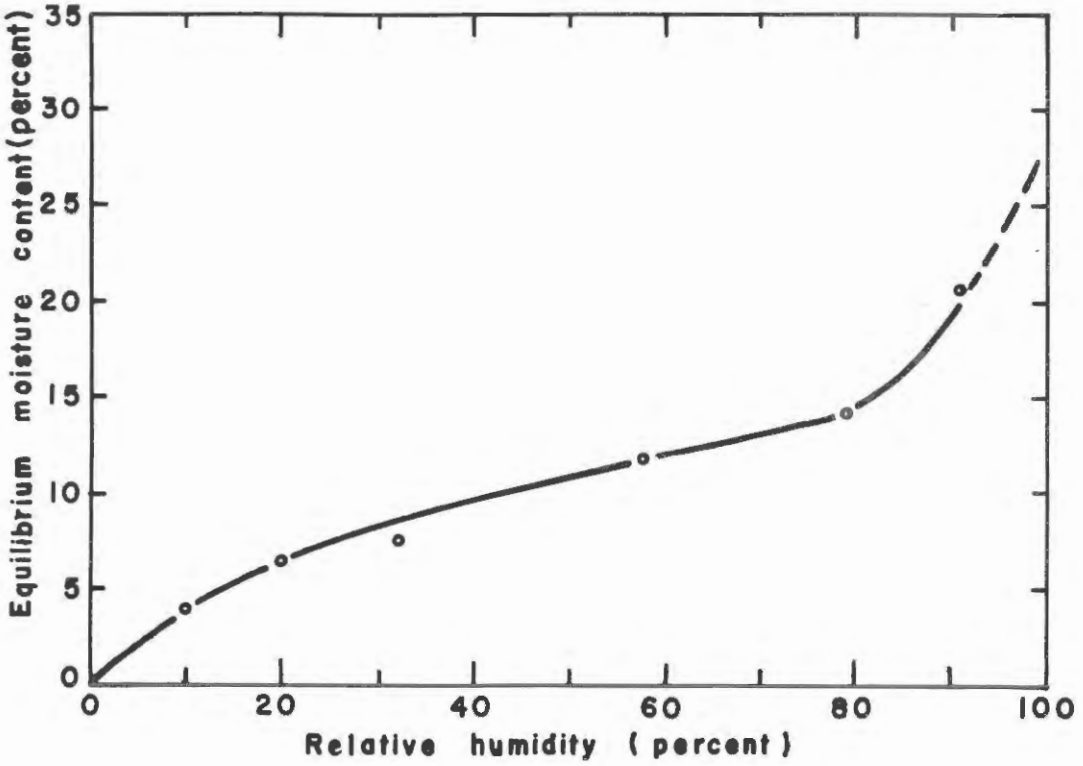

Figure 3. --Relation of the equilibrium moisture content of white fir wood and relative humidity at 70° F.

3. Crib Fire with Side Airflow Restricted

It was found earlier (Fons et al., 1960) that rate of spread through cribs increased only a slight amount with an increase of crib width. This suggested that heat losses from the sides of the crib are negligible in controlling rate of spread. To determine whether the airflow through the sides of the crib affects rate of spread, one test was carried out in which half the length of the crib had the sides shielded. This was accomplished by pretreating strips of brown wrapping paper with monoammonium phosphate salt solution. The strips of treated paper were glued to both sides of half the length of the crib. The crib was ignited and allowed to burn through the section with the unshielded sides and then to continue burning through the section with sides shielded. The treated paper charred as it entered the flaming zone and remained intact until it reached the glowing zone.

Figure 4 shows no change in the spread of fire through the crib as the fire advanced into the shielded section of the crib.

4. Influence of Species of Wood on Rate of Spread

The species tested were white fir, magnolia, basswood, and sugar maple, all nonresinous woods; and longleaf pine, a resinous wood. The cribs for these tests were approximately 5.5 inches high, 9.25 inches wide, and 35.5 inches long, made from nominal 1/2-inch square sticks with a spacing of 1.25 inches between sticks in each tier (table 5). Cribs of each species of wood were burned with different densities and at a moisture content of approximately 10.5 percent. Results of these test fires are shown in figure 5. It is evident from figure 5 that basswood has a higher rate of fire spread

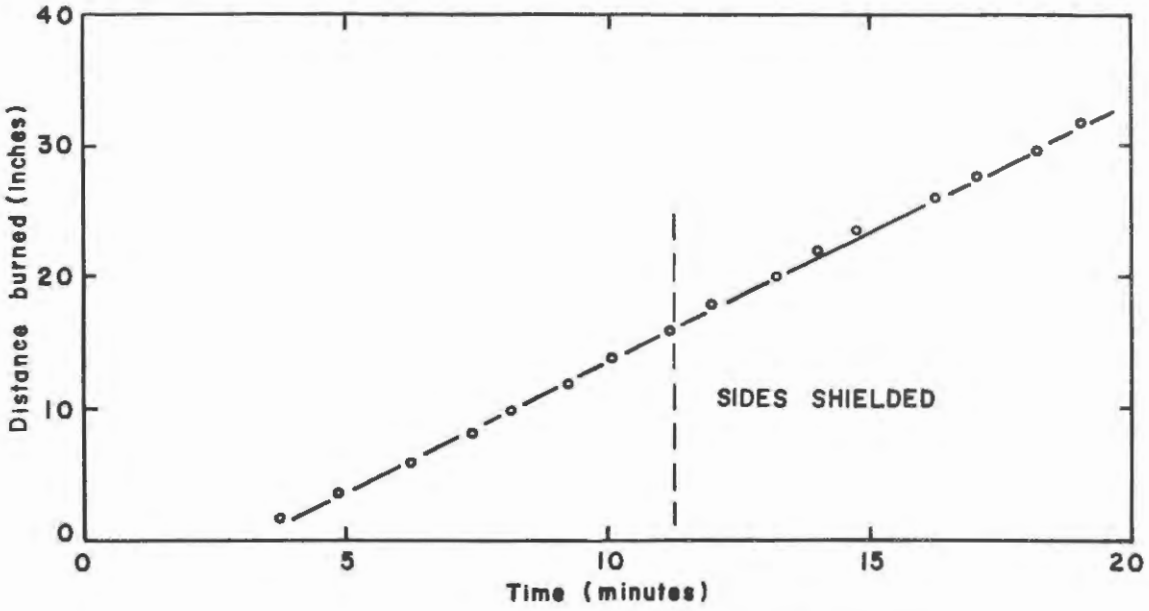

Figure 4. --Spread of fire through a crib of white fir wood, with and without sides shielded.

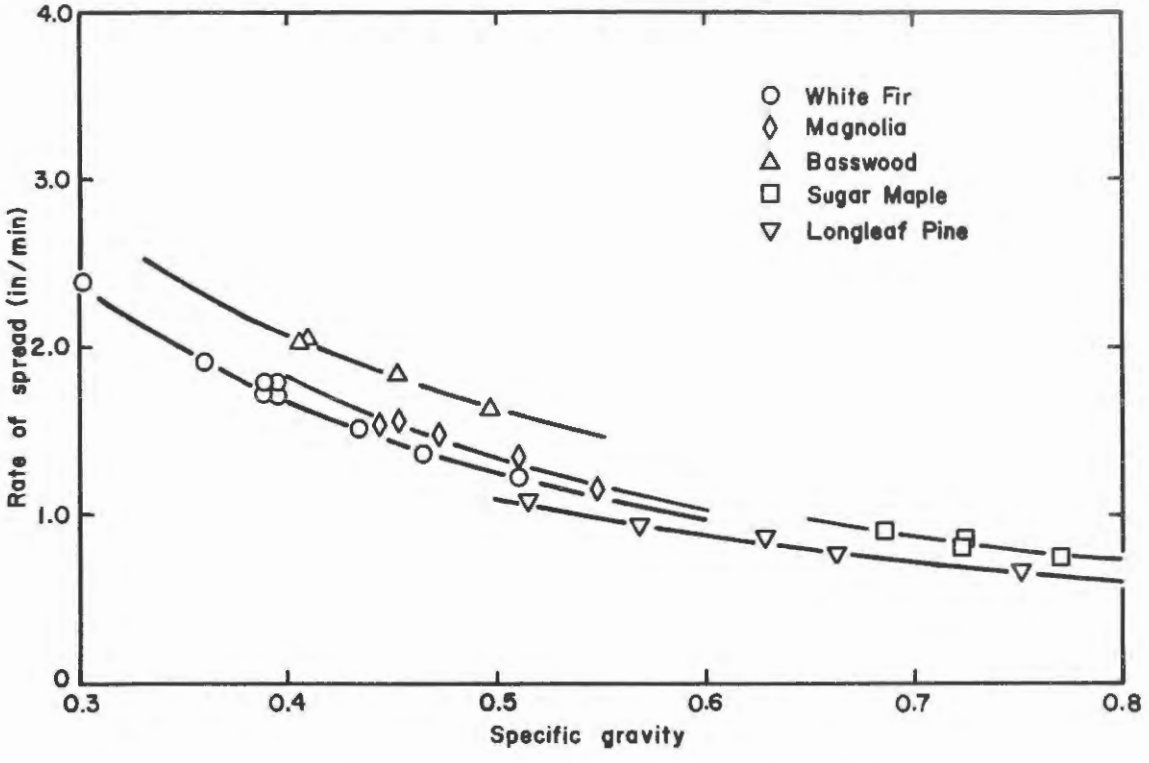

Figure 5. --Rate of fire spread through cribs of wood of different species.

than the other four species. This would indicate that some wood property other than density also has an effect on rate of burning. Basswood has an oil, rich in volatile fatty acids (Wise and Jahn, 1952, p. 563), and this may account for the higher rate of burning. On the other hand, longleaf pine, a resinous wood, has practically the same rate of spread as white fir, maple, and magnolia. The results for longleaf pine indicate that resin in wood does not increase the rate of burning; in fact, it appears to act as a retardant.

5. Influence of Specific Gravity and Moisture Content of Wood on Rate of Fire Spread

Six series of cribs were burned to determine the effect of specific gravity of wood on rate of fire spread for different moisture contents. The cribs were approximately 5.5 inches high, 9.25 inches wide, 35.5 inches long, and made from nominal 1/2-inch square sticks with spacing of 1.25 inches between sticks in each tier (table 4). As shown in figure 6, the rate of spread increases rapidly with decreasing moisture content for specific gravities less than 0.45 and moisture contents less than 10 percent. Since litter, bark, moss, grass, leaves, and partially decomposed wood have specific gravities somewhat less than 0.45 and are the fuels which contribute largely to the spread of most forest fires, it is apparent that moisture content and specific gravity of these fuels are important.

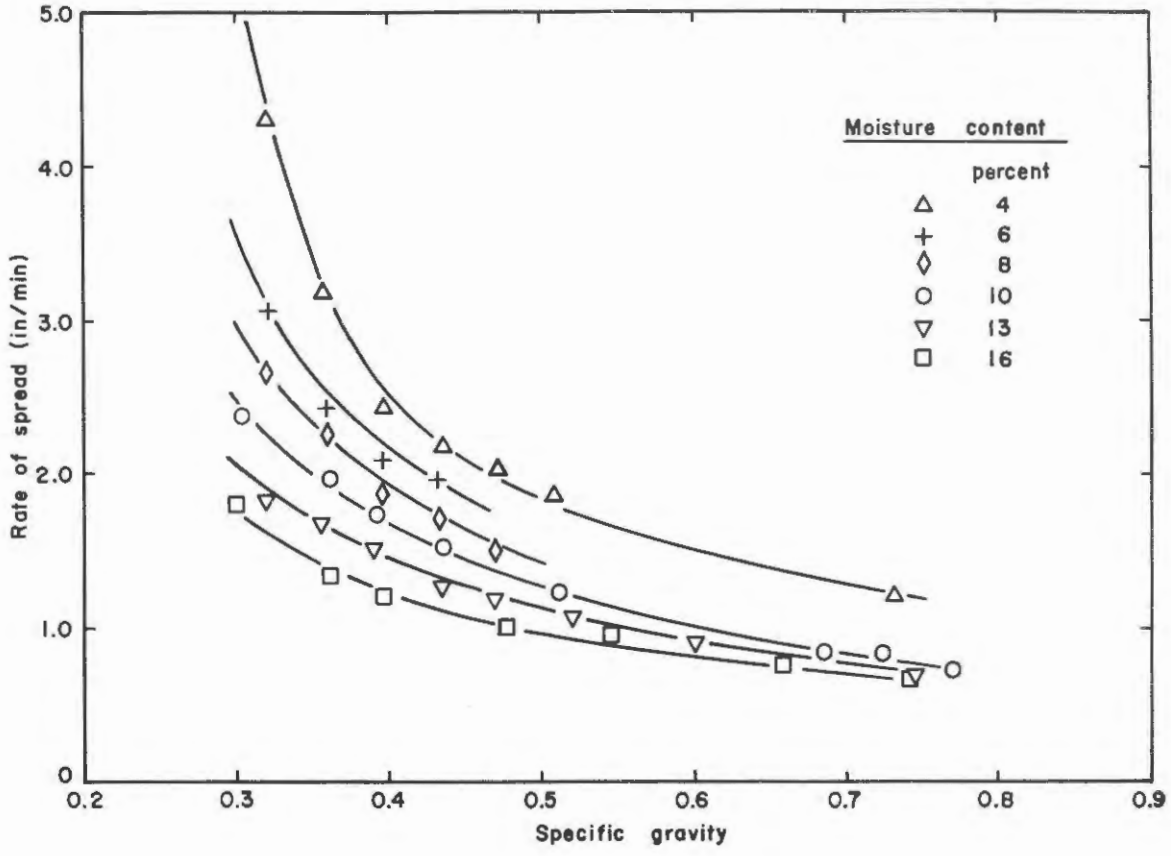

Figure 6.--Effect of specific gravity of wood on rate of spread through cribs at different moisture contents.

6. Flame Dimension Correlation

When buoyant combustible gases emerge from a burning fuel bed into an unconfined atmosphere where they burn as a flame, the rate of oxygen diffusion into the gaseous fuel stream determines the length of the flame. For free-convection fires this diffusion of oxygen controls the rate of burning of the fuel per unit area of the burning zone. A detailed derivation of a simple dimensionless relationship between flame dimensions and rate of burning for buoyant diffusion flames, including a discussion of the work of others, can be found in the paper by Thomas et al., (1961).

The derived dimensionless relationship of the flame dimensions with the modified Froude number containing the combustion gas velocity, V, is

$$\frac{L}{D} = f\left(\frac{V^2}{gD}\right) \tag{1}$$

Assuming that the temperature of the combustion gases emerging from the fuel in the flaming zone is the same for the different fires and that it is equal to the flame temperature of 1650° F., then the velocity, V, of the gases is calculated by the relation

$$V = \frac{CG}{\rho_g} \tag{2}$$

The term, C, is the weight of gas produced per unit weight of solid fuel. For conditions of complete combustion (Kawagoe, 1958), no

excess air, and gas temperature at 1650° F., C = 6.13, and ρ_g = 0.019 lb/ft^3. The flame dimensions can be expressed in terms of the rate of burning per unit area, G, by combining equations 1 and 2

$$\frac{L}{D} = f\left(\frac{C^2G^2}{\rho_g^2 gD}\right) \tag{3}$$

From time-lapse motion pictures taken during the steady-state burning period, measurements of flame length, L, and depth of flaming zone, D, were made of 66 crib fires. These cribs were of varying widths and heights and contained wood of varying densities, fuel sizes, and moisture contents; but, in this flame dimension correlation it is assumed that the fuel and fuel bed parameters are important only in their effect on G, the rate of burning. The rate of burning per unit area, G, of each crib was calculated by the equation

$$G = \frac{WR}{D} \text{ (lbs/ft}^2\text{min)} \tag{4}$$

Since for most of the fires burned, the ratios of the flaming zone, D, to the width of the crib, w_b, were less than 1.0, i.e., $D/w_b < 1.0$, then the advancing flaming zone for these fires may be considered, ideally, a semi-infinite strip or line fire. Dimensionless correlation of flame dimensions with burning rate for crib fires is shown in figure 7 and the equation for the line is

$$\frac{L}{D} = 4.5\left(\frac{C^2G^2}{\rho_g^2 gD}\right)^{0.43} \tag{5}$$

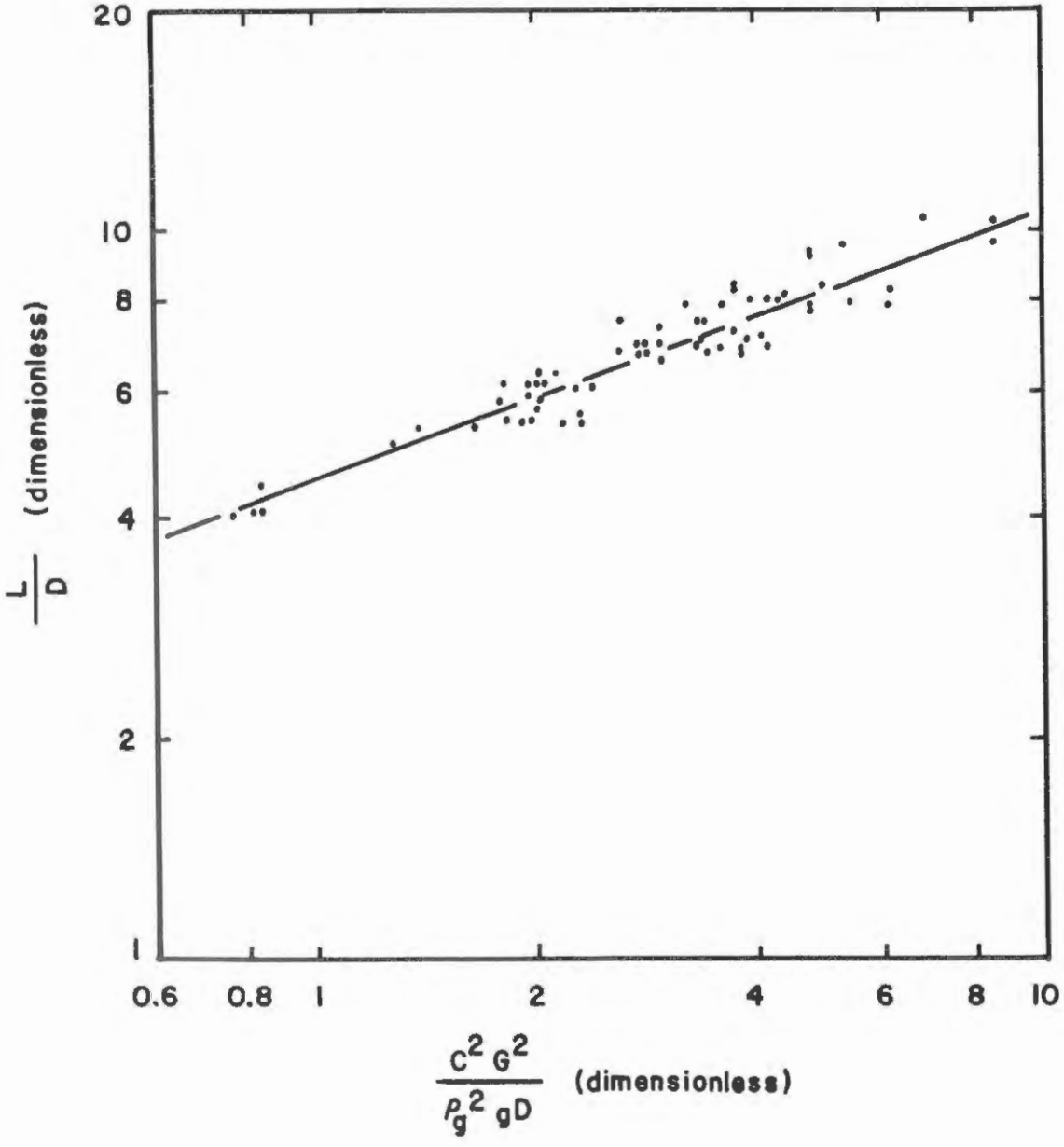

Figure 7. --Dimensionless correlation of flame dimensions with burning rate for crib fires.

The exponent, 0.43, in equation 5 is in agreement with the value found by Thomas (1961) for line fires which were burned both with and without wind. This suggests that the functional power relationship between flame dimensions and Froude number is independent of wind.

Data from fires with $D/w_b < 0.5$ were used to determine the relationship between the flame length, L, and the energy liberation rate per unit length of fire front, HWR. Figure 8 shows that L is proportional to the two-thirds power of HWR. The value of 2/3 is in agreement with that indicated by Thomas[2/] for strip or line fires. The equation for the line is

$$L = 0.74(HWR)^{2/3} \text{ (inches)} \tag{6}$$

where W is expressed in lbs/in^2.

7. Burning Time Correlation

A flaming zone of depth, D, moving at a rate, R, through a fuel bed of solid fuel particles, will require a time, θ_r, to pass a reference point in the fuel bed. During this time, θ_r, a quantity of fuel, W, is burned at a rate, G. Thus, by definition

$$\theta_r = \frac{D}{R} = \frac{W}{G} \tag{7}$$

If the position of a fuel particle is used as a reference point, then θ_r will be the time during which a fuel particle resides in the flaming zone and may be referred to as residence time. This fuel particle

2/ Thomas, P. H. Size of flames from natural fires. The Ninth International Symposium on Combustion. 1962.

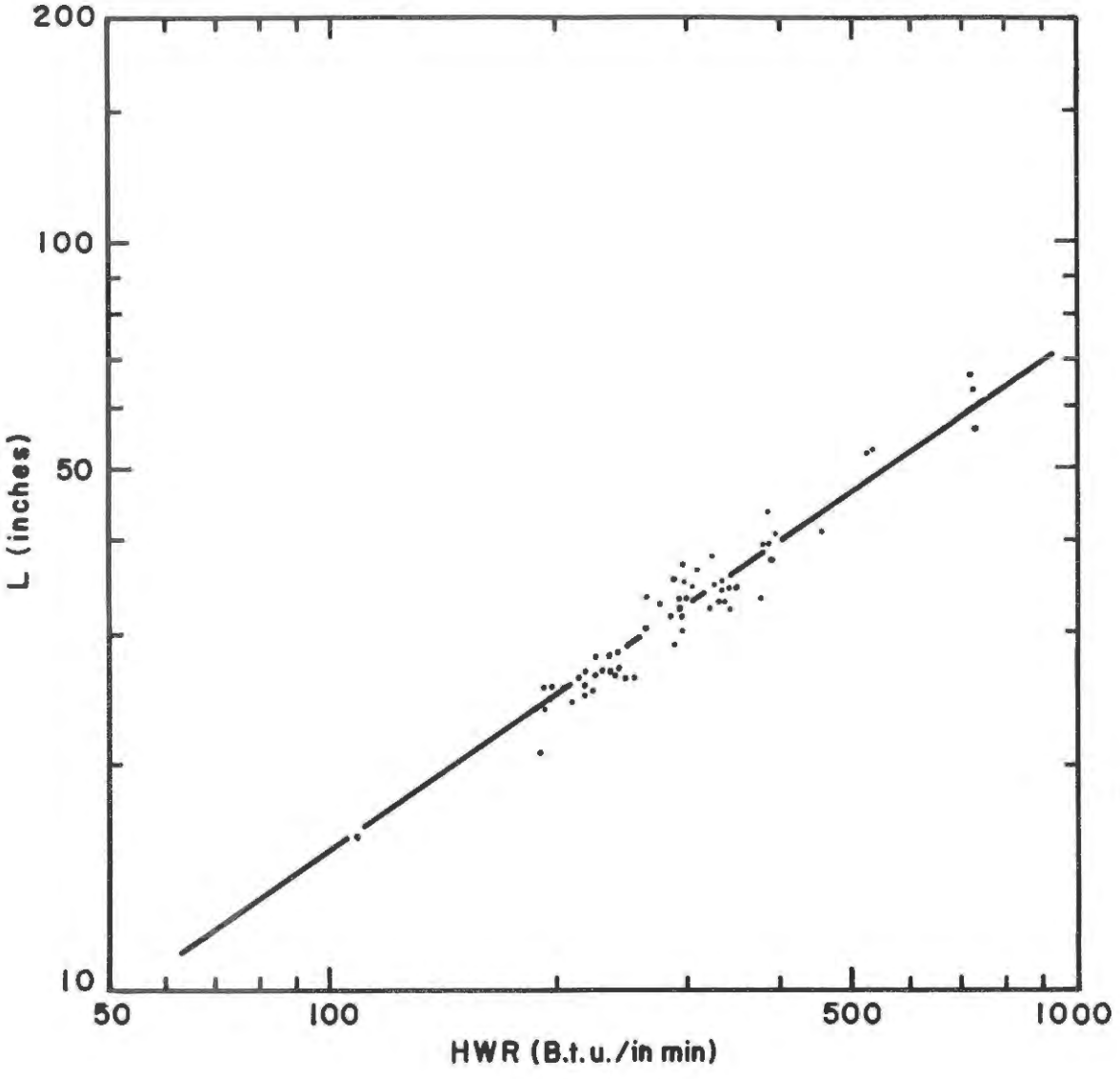

Figure 8. --Flame length as a function of rate of energy released per unit length of fire front.

of initial thickness, d_o, when ignited, is at the front of the flaming zone and is surrounded by a gas at temperature, t_g. The gas is emitted by the burning particles spaced at regular intervals from each other. At ignition, the center of the particle is at temperature, t_o, and its temperature increases with time until the particle reaches the rear of the flaming zone. It is assumed that when the particle arrives at the rear of the flaming zone all of its volatiles are released and its center reaches the same temperature as that of the surrounding gas. It is also assumed that at the burning surface the mass transfer of the volatiles from the burning particle is proportional to the heat transfer by conduction into the particle. This presupposes that the mass diffusivity is proportional to the thermal diffusivity. The heat flow to the burning particle from the neighboring burning particles is proportional to hd_o/k_g. Since the temperature of the surrounding gas is assumed to be constant, it follows then that the ratio h/k_g is effectively constant. The temperature, t_g, of the gas will depend on its heat capacity and the amount of heat transferred to it by the burning particles of the combustion zone less the losses by convection to the atmosphere. For steady-state conditions, it is assumed that the gas temperature, t_g, and density, ρ_g, remain constant and have the values of 1650° F. and 0.019 lb/ft^3, respectively (Kawagoe, 1958).

Consider a flaming zone moving through a fuel bed of height, h_b, width, w_b, and composed of fuel particles with initial thickness, d_o, moisture content, M_f, and density, ρ_f. At time, θ, after the particle enters the flaming zone, the temperature, t, at the center of a particle may be determined by an equation which expresses the fuel and

fuel bed parameters and the mass and energy transfer rates in terms of dimensionless groups. The equation is written as

$$\frac{t - t_o}{t_g - t_o} = f\left(\frac{\theta\alpha}{d_o^2}, \frac{L}{D}, \frac{k_g}{hd_o}, \frac{\rho_f}{\rho_g}, M_f, \frac{h_b}{w_b}, \frac{V_g}{V_f}, \frac{4h_b}{d_o}, \frac{D}{d_o}\right) \qquad (8)$$

The first two dimensionless groups on the right side of equation 8 are, respectively, Fourier number and the length and depth of flame ratio; the latter is a function of Froude number as presented in the preceding section. Fourier number describes the heat transfer by conduction into a solid body from its surface and in this analysis it is assumed to be proportional to mass transfer (Spalding, 1955). Froude number, in this case, represents the natural convective heat and mass transfer from a source to the atmosphere. The third dimensionless group, k_g/hd_o, is the reciprocal of Nusselt number, which describes the heat transfer between the surface of the particle and the surrounding gas. If k_g/h is assumed to remain constant during the burning of a particle of initial size, d_o, then the dimensionless group $k_g h/d_o$ may be considered as an independent parameter. The remaining six groups of equation 8 are ratios involving fuel and fuel bed parameters.

It follows that when $\theta = \theta_r$, then $t - t_o = t_g - t_o$ and equation 8 may be written as

$$\frac{\theta_r \alpha}{d_o^2}, \frac{L}{D} = f\left(\frac{k_g}{hd_o}, \frac{\rho_f}{\rho_g}, M_f, \frac{h_b}{w_b}, \frac{V_g}{V_f}, \frac{4h_b}{d_o}, \frac{D}{d_o}\right) \qquad (9)$$

In equation 9, if θ_r is replaced by D/R from equation 7, then the left side becomes $L\alpha / Rd_o^2$. Similarly, replacing θ_r with W/G in equation 9, the left side becomes $WL\alpha / GDd_o^2$. The product GD is the rate of burning per unit width of a line fire.

To determine the numerical value of the dimensionless group $\theta_r \alpha / d_o^2$, α is replaced by $k/\rho_f C_p$ and θ_r is replaced by D/R (equation 7). For each fire, measurements of the width of flaming zone, D, are taken from 3-second time-lapse motion pictures. Thermal diffusivity, α, is determined by using an empirical equation for thermal conductivity, k, expressed as a function of density, ρ_f, of bone-dry wood (MacLean 1941), and a value of 0.327 is used for the specific heat, C_p, of bone-dry wood (Dunlap 1912). When ρ_f is expressed as lbs/ft^3, the equation for α in units of inches squared per minute becomes:

$$\alpha = \frac{0.100}{\rho_f} + 0.0137 \qquad (10)$$

Data from 106 fires, including 22 stationary flame model fires by Gross (1962), were analyzed to establish exponents for the dimensionless ratios on the right side of equation 9. For fires by Gross, D/d_o was held constant at a value of 10. For the propagating flame model in which the depth of the flaming zone is allowed to assume a natural value, data showed that the ratio D/d_o for each fire was approximately 10.5. Since D/d_o remained constant for the two types of models, this group was not considered in the analysis. In the dimensionless group k_g/hd_o, a value of unity was chosen for the ratio k_g/h.

The fires by Gross were used to determine the exponent for V_g/V_f because the ratios h_b/w_b and $4h_o/d_o$ for these cribs were constant and V_g/V_f was varied independently of fuel size. The exponent for k_g/hd_o was determined from data taken on fires in which fuel size, d_o, was varied. For these fires the product of V_f/V_g and $4h_b/d_o$ was held constant. Equation 9 with the exponents for the dimensionless groups becomes

$$\frac{\theta_r \alpha}{d_o^2} \frac{L}{D} = f\left[\left(\frac{\rho_f}{\rho_g}\right)\left(M_f\right)^{0.15}\left(\frac{h_b}{w_b}\right)^{0.1}\left(\frac{h_b}{\lambda}\right)^{0.65}\left(\frac{k_g}{hd_o}\right)^{1.5}\right] \quad (11)$$

where $\lambda = V_g d_o/4V_f$

Based on equation 11, a correlation of the data is shown in figure 9 by the curve which has a slope of unity.

Equation 11 gives the scale effects of the fuel and fuel bed variables on burning time, propagating rate, and burning rate for crib fires. With the exception of the gas-to-fuel-volume ratio, the range of fuel and fuel bed variables covered by the crib fires is comparable to those sometimes found in forest areas. For most forest fuel types, such as grass, litter, and brush, the gas-to-fuel-volume ratio (V_g/V_f) is greater than 4.0 (Fons, 1946). Equations 6 and 11 may be used to make quantitative estimates of flame length, L, rate of propagation, R, and rate of burning per unit width, GD, for line fires in forests.

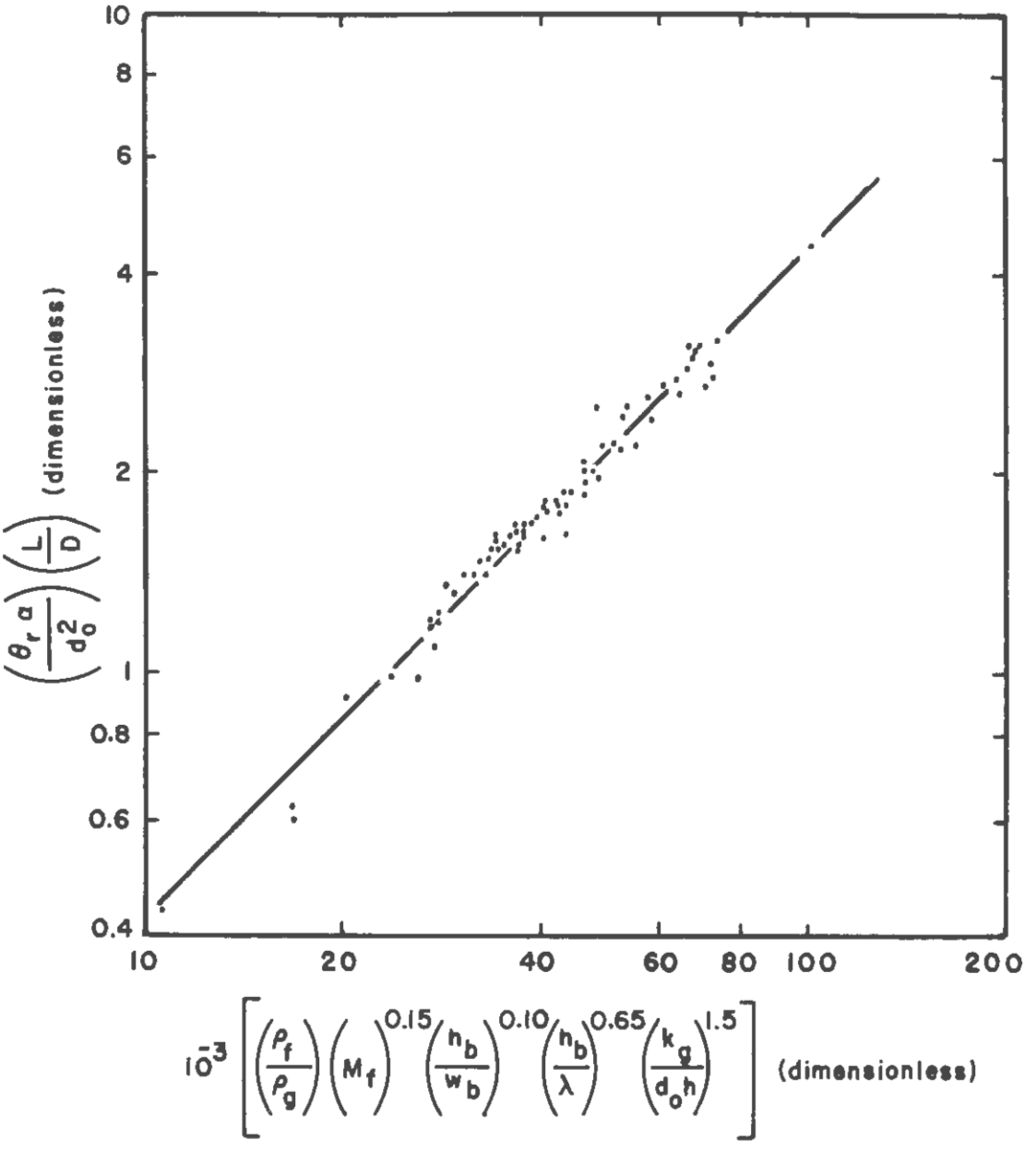

Figure 9. --Dimensionless correlation of heat and mass transfer with fuel and fuel bed parameters for crib fires.

8. Convective Heat

The rate of convective heat, Q_c, from crib fires is determined by the mass velocity of the gas through the exhaust stack, the specific heat of the gas, and the terminal temperature difference between the stack gas and the incoming air. The equation for calculating the rate of convective heat is

$$Q_c = A_s \bar{U} \rho_s C_p' \Delta t \qquad (12)$$

For each crib fire the maximum stack velocity, U_{max}, is measured with a Pitot tube at a position six diameters above the entrance. A ratio of $\bar{U}/U_{max} = 0.89$ was established from results of a traverse made across the section of the stack for a Reynolds number of 0.25×10^6. Thus, equation (12) becomes

$$Q_c = 0.89 U_{max} A_s \rho_s C_p' \Delta t \qquad (13)$$

Equation 13 neglects heat lost through the hood and the stack wall. The temperature difference, Δt, between the stack gas and the incoming air for each fire is measured directly with a parallel-series arrangement of thermocouples. Four thermocouples, wired in parallel and placed six feet above the floor at the four corners of the combustion table, sense the temperature of the incoming air. In series with these is connected a fifth thermocouple which is peened at the center of a 1/4-inch copper tube and placed across the stack 12.5 feet above the entrance. It is assumed that the copper tube attains the average temperature of the stack gases soon after a steady-state burning condition is established for a crib fire.

Figure 10 shows that the rate of convective heat, Q_c, calculated by equation (13), is proportional to the rate of combustion, Q. The rate of combustion is determined by the following equation:

$$Q = \frac{HGw_b L_b}{8640} \quad \text{(Btu/sec)} \tag{14}$$

9. Radiative Heat

a. Irradiance.--The irradiance of the crib fires was measured by directional thermopile radiometers at three different positions (fig. 11). The radiometer distance of 18.57 feet from the flaming zone was more than adequate to permit the hot-junction receiver strip to see the combined area of the burning zone within the crib and the flaming zone above the crib. Detailed description of the directional radiometer is given in reference (Gier and Boelter, 1941, pp. 1284-1292). Briefly, the radiometer consists of a 150-junction, silver-constantan thermopile mounted in the rear of a cylindrical metal housing. A rear plate with a narrow slot allows radiation entering the front opening of the radiometer to impinge on the hot-junction receiver strip, while shielding the cold-junction strip. The output of the thermopile is linear. A calibration factor, K, in Btu/ft^{2}hr per millivolt output is furnished for each instrument by the manufacturer.

Tables 8 and 9 in Appendix A give irradiance measured at three positions (front, rear, and side of fire) for 57 fires. Figure 12 shows irradiance, I, as a function of rate of combustion, Q. The results shown in figure 12 indicate that the irradiance at the side and rear of the crib fires are approximately equal. The results also show that the irradiance at the front of the fire is about 60 percent of the

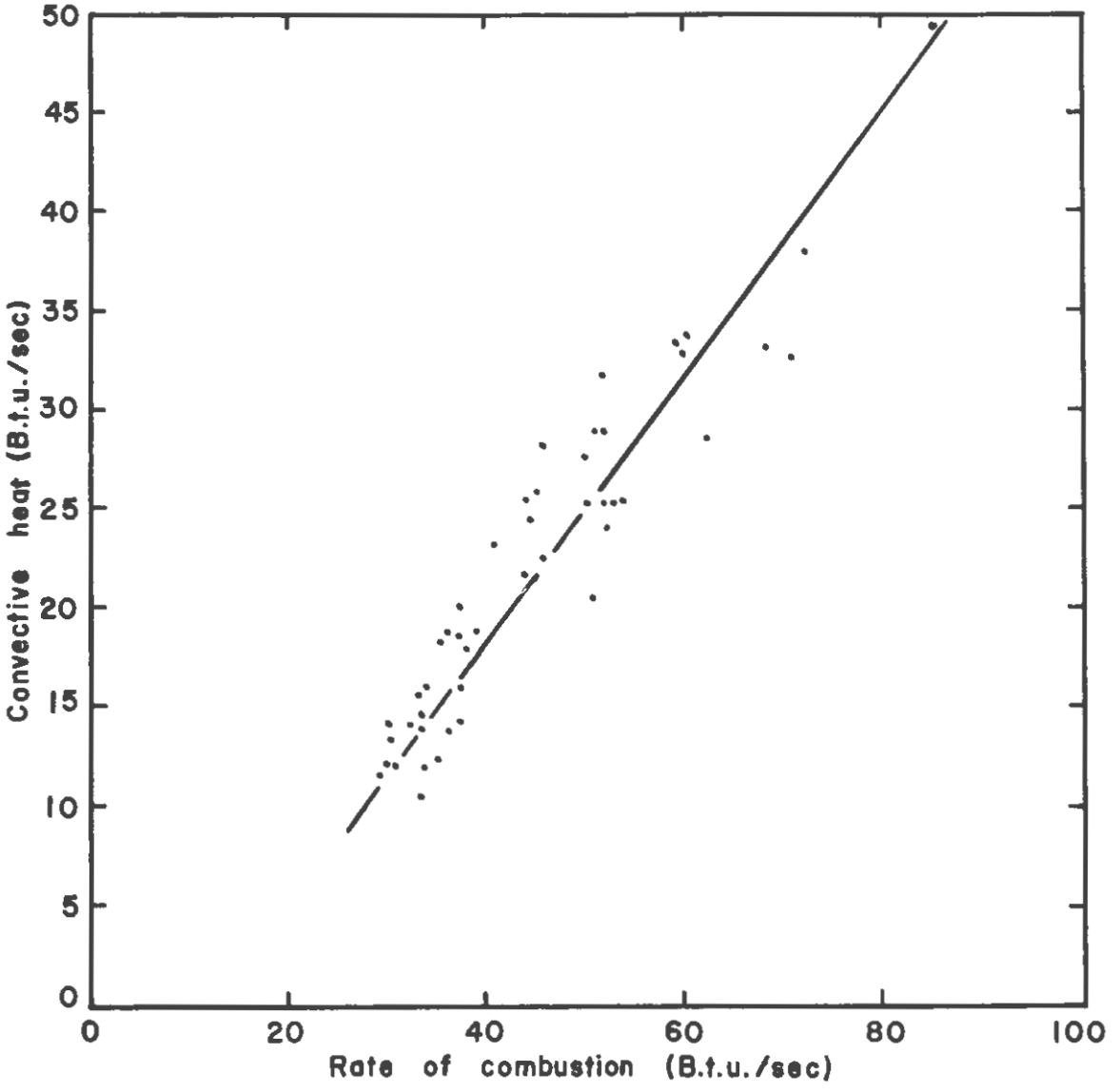

Figure 10. --Rate of convective heat, Q_c, of crib fires with different rates of combustion, Q.

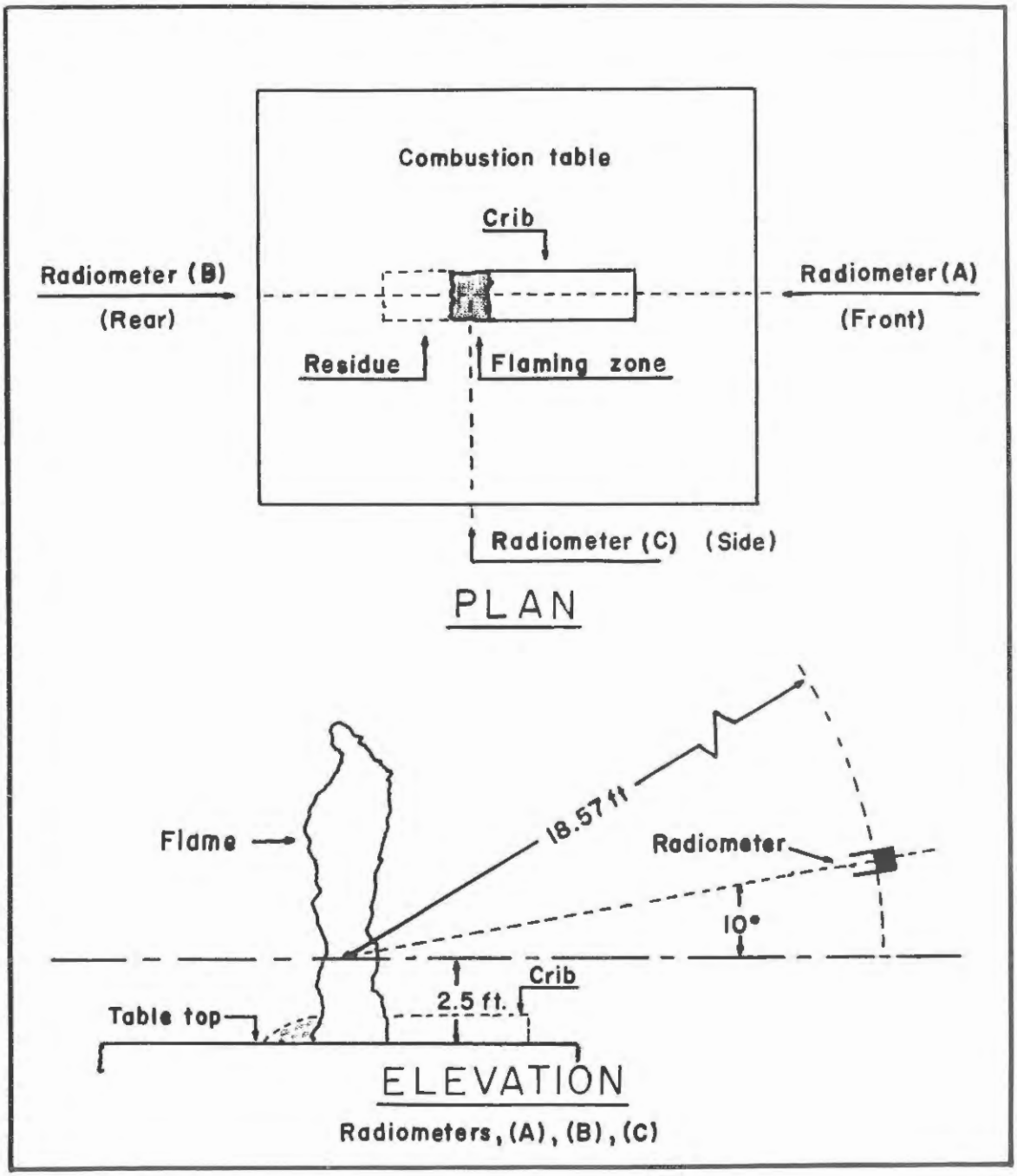

Figure 11. --Schematic diagram, illustrating positions of radiometers relative to crib and flaming zone.

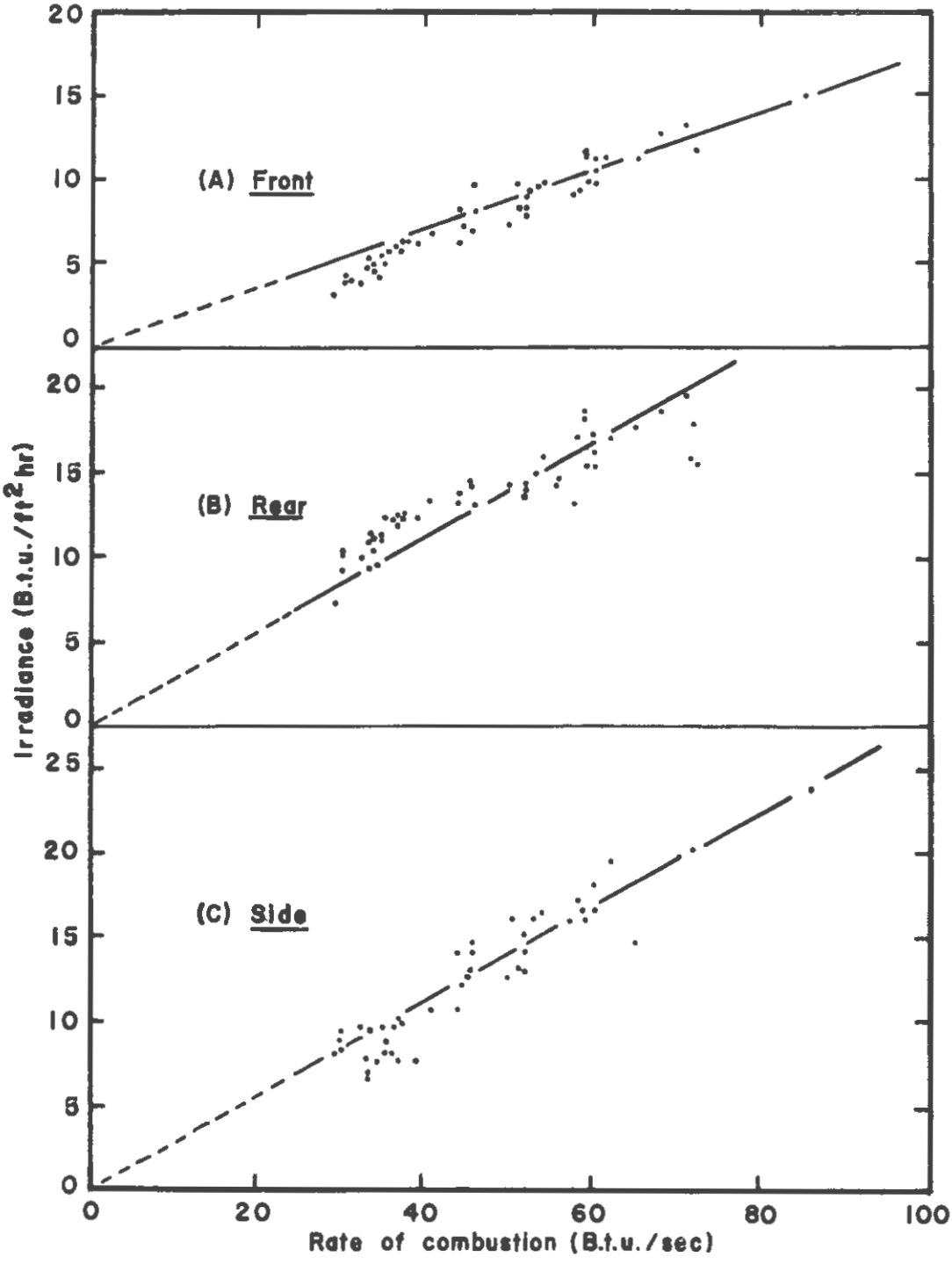

Figure 12.--Irradiance, I, at three positions, as a function of rate of combustion, Q.

irradiance measured at the side or rear. The decrease in irradiance at the front of the fire may be accounted for by the fact that the burning zone within the crib is shielded from the radiometer by the unburned portion of the crib, (see figure 11, radiometer position (A)). This suggests that the burning zone within the crib contributes about 40 percent of the irradiance toward the unburned fuel.

b. Rate of Radiative Heat.--Measurements of the irradiance were made at several points for determining the rate of radiative heat. These measurements were made for fires in cribs of different species of wood, (see table 5). For these fires the three radiometers at positions (A), (B), and (C) in figure 11 were mounted on carriages which could be moved along a curved standard to various elevation angles, ranging from -15° to $+50^{\circ}$, (Fons et al., 1959). The radius of curvature for the standard was 14 feet with the origin at a point in the flame 2 feet above the base of the fuel bed. The horizontal or zero position of the radiometer angle, therefore, corresponds to the base of a hemisphere with a radius of 14 feet. Readings for each radiometer were taken at angles of 0°, 10°, 20°, 30°, 40°, and 50° during the steady-state burning period of a fire. Irradiance data for each of the three positions were plotted against elevation angles from 0° to 50°. The curves drawn through the points were extended to -10° and 90° to approximate the irradiance below 0° and above 50°. This method of approximating the irradiance above 50° should not seriously affect the final result because the surface area of the hemisphere from 50° to the zenith or 90° is only 15 percent of the surface area used in calculating the total radiant energy. The cutoff angle imposed by

the combustion table on the radiometers was about 8° below the horizontal, so radiant energy from -8° to -90° was not included in the integration procedure. It is assumed that the radiant energy intercepted by the top of the combustion table is transferred to the entrained air as convective heat.

Irradiance measurements from the front and rear radiometers were used to calculate the radiative heat for 1/2 of the surface area or 1/4 each of the partial sphere -8° to $+90^{\circ}$ in the integrating procedure. The measurements from the side radiometer were used in computing the radiative heat for the remaining half of the surface area. Estimates of rate of radiative heat, Q_r, obtained by the integration method are presented in table 2. The average rate of radiative heat, Q_r, for the 15 fires is approximately 17 percent of the average rate of combustion, Q.

Table 2.--Rate of radiative heat from crib fires

Fire No.	Q_r	Fire No.	Q_r
	Btu/sec		Btu/sec
1M	7.66	3S	5.55
3M	8.12	4S	5.27
4M	7.58	1Y	6.28
5M	8.28	2Y	6.08
2B	8.88	3Y	6.14
3B	8.45	4Y	5.52
4B	8.24	5Y	5.41
5B	9.22		

10. Flame Emissivity

The emissive power, E_b, from a black body or an ideal radiator at temperature, T, may be expressed by the Stefan-Boltzmann equation as

$$E_b = \sigma T^4 \tag{15}$$

Thus, if E_b is the emissive power from a black body, the emissivity of a non-black body, with an emissive power, E, may be defined as

$$\epsilon = \frac{E}{E_b} \tag{16}$$

For a diffuse surface, equation (16) may be considered to define the total or mean effective emissivity with respect to radiation from a surface at any angle. Combining equations (15) and (16) gives

$$\epsilon = \frac{E}{\sigma T^4} \tag{17}$$

The equation for calculating the emissivity of a flame from radiometer measurements must consider the radiant energy exchange between the flame and the radiometer receiver strip. For this purpose the equation must include the geometrical view factor between the receiver strip and the flame surface. The shape of the flaming zone of a crib fire is nearly rectangular when viewed from the side, front, or rear (fig. 1). Tables of view factors for rectangular sources, to a point in a plane parallel and to a point in a plane perpendicular to the source, are presented in Appendix B, tables 10 and 11.

The radiometer, at the position of zero degrees, sees a circular area (Gier and Boelter, 1941, pp. 1284-1292) within which is a nearly rectangular flaming surface in a plane parallel to the radiometer receiver strip. The irradiation of the radiometer receiver strip, considered as an incremental area, ΔA_1, is composed of several parts:

1. Energy emitted by flame surface of area, A_2, at temperature, T_2, is $\epsilon_2 F_{21} A_2 T_2^4$.

2. Energy emitted by an area, A_3, at temperature, T_3, within the circular area viewed by the radiometer with A_2 excluded is $\epsilon_3 F_{31} A_3 T_3^4$.

3. Energy emitted by the surroundings at temperature, T_4, and reflected from A_2 is $(1 - \epsilon_2) \epsilon_4 F_{21} A_2 T_4^4$.

4. Energy emitted by the surroundings at temperature, T_4, and reflected from A_3 is $(1 - \epsilon_3) \epsilon_4 F_{31} A_3 T_4^4$.

5. Energy emitted by the receiver strip to area, A_2, is $- \epsilon_1 F_{12} \Delta A_1 T_1^4$.

6. Energy emitted by the receiver strip to area, A_3, is $- \epsilon_1 F_{13} \Delta A_1 T^4$.

It is assumed that $T_1 = T_3 = T_4$, $\epsilon_1 = \epsilon_3 = \epsilon_4 = 1$, and that by the reciprocity theorem $F_{12} \Delta A_1 = F_{21} A_2$ and $F_{13} \Delta A_1 = F_{31} A_3$. Adding the energies emitted by the several parts gives an expression for irradiation

$$K\,(mv) = \epsilon_2 F_{12} (T_2^4 - T_1^4) \qquad (18)$$

where (mv) is the millivolt output of the radiometer and K is its calibration factor in Btu/ft^{2}hr per millivolt.

Solving equation (18) for ϵ_2 the emissivity of the flame is

$$\epsilon_2 = \frac{K(mv)}{F_{12}(T_2^4 - T_1^4)} \qquad (19)$$

The product, K(mv), in equation (19) is equivalent to the emissive power, E, of a surface given by equation (17).

Values of K(mv) were calculated from radiometer millivolt output, (mv), for rear and side positions of 30 crib fires. The corresponding view factors, F_{12}, were determined by table 10 from the measured flame dimensions of each fire. Flame temperature of each fire was assumed constant at 1600° F. for the entire flame zone.

Table 3 presents the emissivities calculated by equation 19, ϵ_r (rear view) and ϵ_s (side view), of 30 fires; also, included in table 3 are ratios of flaming zone depths, w_b/D, and ratios of emissivities, ϵ_r/ϵ_s. In comparing the ratios of w_b/D with ϵ_r/ϵ_s, it appears that for crib fires the emissivity is proportional to the depth of flame.

11. Temperature of Convection Column

Temperatures of the convection column from crib fires were measured with 33 No. 30 chromel-alumel (bare) thermocouples arranged in three grids at levels of 47, 76, and 120 inches above the combustion table. Typical curves showing the horizontal distribution of temperatures at the three levels and the vertical temperature distribution along the central axis were presented in an earlier paper (Fons et al., 1959).

Table 3.--Emissivities for flames of crib fires

Fire No.	Rear view [1]			Side view [1]			w_b/D [2]	ϵ_s/ϵ_r
	K(mv)	$F_{12} \times 10^4$	ϵ_r	K(mv)	$F_{12} \times 10^4$	ϵ_s		
	$\frac{Btu}{ft^2 hr}$	--	--	$\frac{Btu}{ft^2 hr}$	--	--	--	--
31	15.0	22.8	0.213	14.8	11.8	0.407	1.85	1.91
32	13.8	25.2	.177	15.4	14.4	.347	1.71	1.96
33	13.0	26.4	.160	14.0	15.0	.304	1.74	1.90
34	13.2	27.2	.157	14.2	14.2	.324	1.81	2.06
35	17.4	29.6	.191	20.1	33.8	.193	0.86	1.01
37	13.2	22.0	.194	13.4	11.6	.376	1.93	1.94
38	14.4	24.4	.191	14.4	17.4	.270	1.38	1.41
39	13.0	23.6	.179	13.6	12.2	.362	1.81	2.02
40	13.6	23.6	.187	14.0	12.2	.373	1.85	1.99
41	11.6	21.8	.173	12.0	10.4	.374	2.01	2.16
42	12.8	23.4	.177	13.8	12.2	.366	1.89	2.07
44	11.2	22.2	.164	12.6	10.6	.385	2.06	2.35
45	12.2	23.4	.170	13.0	13.2	.320	1.78	1.88
46	9.5	18.8	.164	8.2	9.0	.297	2.10	1.81
47	8.5	18.0	.153	7.8	8.6	.295	2.06	1.93
48	8.5	17.6	.157	8.0	8.4	.309	1.97	1.97
50	8.5	17.6	.157	8.4	8.4	.325	2.15	2.07
51	8.0	18.2	.143	7.2	7.8	.301	2.31	2.10
52	10.1	19.4	.169	8.2	9.4	.285	2.01	1.69
53	10.4	19.8	.171	8.6	9.4	.297	2.06	1.74
54	10.6	18.8	.184	8.4	9.2	.297	2.06	1.61
55	9.7	18.6	.169	8.2	9.0	.297	2.01	1.76
56	8.8	17.6	.162	6.6	7.6	.283	2.26	1.75
57	9.7	19.4	.162	7.6	8.4	.296	2.26	1.83
59	15.8	20.4	.252	13.6	12.0	.368	1.71	1.46
60	15.1	23.0	.214	12.4	15.2	.265	1.44	1.24
62	14.7	29.0	.165	14.0	15.2	.300	1.81	1.82
63	15.5	26.4	.190	14.4	13.8	.338	1.89	1.78
64	15.9	28.4	.182	15.4	20.2	.247	1.34	1.36
65	16.7	25.0	.216	19.2	17.8	.350	1.36	1.62

[1] Radiometer position, see figure 11.
[2] w_b, depth of flame side view; D, depth of flame rear view.

The natural convection movement of the heated column above fires is responsible for the air entrainment into the column. To gain a fundamental understanding of the convection zone of a fire burning in a free atmosphere, Scesa and Sauer (1954) and Yih (1953, pp. 117-133) made theoretical analyses of the transport processes for point and line heat sources based on heat transfer and fluid flow theories. Lee and Emmons (1961) made a theoretical analysis and an experimental study of the convection above a line fire with a channel burner using the liquid fuels acetone and methyl alcohol. Yih used Bunsen burners to study convection above a point source.

The equation, giving temperature distribution within a turbulent column above a point source (Scesa and Sauer, 1954), was rearranged into a functional relationship between dimensionless height and dimensionless temperature rise as follows:

$$\frac{Y}{Z} = \phi\left[\frac{\Delta T\, g\, Z^{5/3}}{T_o\,(Q_c/C_p\, T_o\, \rho_o)^{2/3}}\right] \qquad (20)$$

The temperature data of the convection column from 20 fires in cribs 5.5 inches high and 9.25 inches wide were correlated, using the functional relationship given by equation 20. Since these crib fires are finite sources, 1/2 foot was added to the height to adjust values of Z to a vertical distance from a virtual point source. Figure 13 shows the relationship of the two dimensionless groups which characterizes the temperature field of the convection columns resulting from these wood crib fires. The correlation of the two dimensionless groups for the crib fires agrees reasonably well with results obtained by Yih (1953, pp. 117-133).

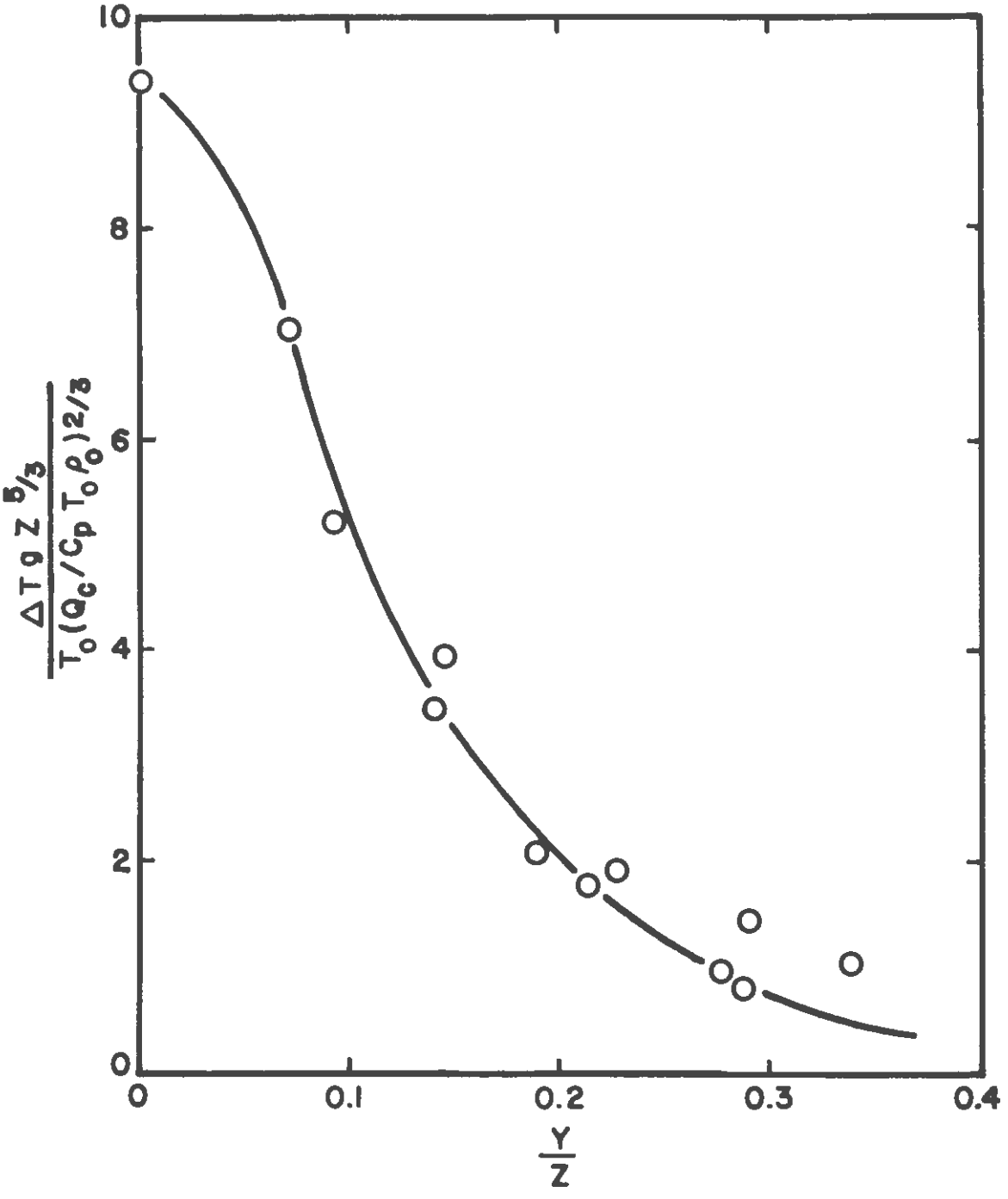

Figure 13. --Temperature distribution function for turbulent convection above crib fires.

CONCLUSIONS

1. Dimensionless relationship between the flame dimensions and modified Froude number, found by others using stationary flame models, is also applicable to a propagating flame model.

2. For line fires the burning rate or the rate of fire spread of a given fuel can be estimated from the flame length.

3. Relationships can be established between the burning characteristics of wood crib fires and the fuel and fuel bed parameters, expressed in dimensionless form, by the power law assumption.

4. The spatial distribution of temperature in the convection column of a wood crib fire is similar to the distribution found for other heat sources.

5. The rate of radiative heat from laboratory crib fires is approximately 17 percent of the total heat rate evolved.

6. In determining the total effective flame emissivity of crib fires, the depth of flaming zone must be considered.

PLANS FOR CONTINUATION

A proposal for the continuation of Project Fire Model was submitted on November 17, 1961, to the Bureau of Standards for consideration. The proposal was approved on February 28, 1962, for a period ending June 30, 1963.

A brief description of the research work proposed to be undertaken follows:

1. To learn the effect of fuel size upon certain dependent variables associated with free-burning fire. The effect of fuel size on rate of spread through white fir wood cribs has been obtained for a range of stick sizes, from 1/4 to 1-1/4 inches square (see page 34, Summary Report, May 31, 1960). These tests were made with density and moisture content of the wood constant, averaging 0.385 and 10.4 percent, respectively. It is proposed to conduct additional tests to include higher and lower densities and moisture contents. Data from such tests should confirm whether or not residence time scales to the three-halves power of fuel size regardless of fuel moisture or density.

2. To learn the effect of particle spacing in the fuel bed on fire characteristics. Earlier work on fire spread with beds of natural fuels indicated that rate of spread increased as the ratio of voids to the fuel surface area in the fuel bed increased.

   The spacing of sticks making up the cribs tested on the project thus far has been kept at a constant value of 1-1/4 inches on the horizontal plane; on the vertical plane the spacing has been equal

to the thickness of the sticks. It is proposed to test cribs of 1/2-inch square sticks of white fir with spacing varied from 1/2 to approximately 3 inches. Present method of crib construction will be modified to obtain equal spacing in the vertical and horizontal plane regardless of stick sizes.

3. To relate the properties of free-burning fire in wood-crib fuel beds to independent variables affecting the fire. Analysis of the phenomenon of combustion of beds of solid fuels will be continued to explain such behavior aspects as rate of spread, partition of energy, and convection column characteristics. The ultimate objective of these analyses will be to develop through theory and from experimental data obtained from model fires scaling laws for prediction of the behavior and properties of full-scale free-burning fires.

NOMENCLATURE

Symbol	Description	Units
A_s	Cross-sectional area of exhaust stack	ft^2
C	Mass of combustion gas produced per unit mass of solid fuel	----------
C_p	Specific heat of dry wood; also specific heat of ambient air	Btu/lb^oF
C_p	Specific heat of stack gas at constant pressure	Btu/lb^oF
d_o	Initial thickness of fuel	inches
D	Depth of flaming zone in the direction of fire spread	inches
E	Emissive power of a non-black body	Btu/ft^2hr
E_b	Emissive power of a black body	Btu/ft^2hr
F_{12}	View factor from area 1 to area 2	----------
g	Acceleration due to gravity	ft/sec^2
G	Rate of fuel burning per unit area	lbs/ft^2min
h	Heat transfer coefficient	Btu/ft^2hr^oF
h_b	Height of fuel bed	inches
H	Low heat value of dry wood	Btu/lb
I	Irradiance, intensity of radiation	Btu/ft^2hr
k	Thermal conductivity of dry wood	$Btu/ft\ hr^oF$
k_g	Thermal conductivity of gas surrounding the fuel particle	$Btu/ft\ hr^oF$
K	Radiometer calibration factor	Btu/ft^2hr per millivolt
L	Length of flame	inches
L_b	Length of fuel bed	inches

m	Mass of water in fuel	lbs
m_f	Mass of bone-dry fuel	lbs
M_f	Moisture content, $100m/m_f$	percent
Q	Rate of combustion	Btu/sec
Q_c	Rate of convective heat	Btu/sec
Q_r	Rate of radiative heat	Btu/sec
R	Rate of fire propagation	in/min
t	Fuel temperature at center of fuel particle	^oF
t_g	Gas temperature in the flaming zone	^oF
t_o	Room temperature; also initial temperature of the fuel	^oF
t_s	Stack gas temperature	^oF
T	Temperature, absolute	^oR
T_o	Temperature of ambient air	^oR
$\bar{U}$	Average stack gas velocity	ft/sec
U_{max}	Maximum stack gas velocity; measured at the center of stack	ft/sec
V	Vertical velocity of combustion gases emerging from the flaming zone	ft/sec
V_f	Volume of fuel in crib	in^3
V_g	Volume of gas or void in crib	in^3
w_b	Width of fuel bed; also depth of flame (side view)	inches
W	Weight of fuel burned per unit area	lbs/ft^2
W_f	Weight of fuel in crib	lbs
W_o	Loading, weight of fuel in crib per unit area	lbs/ft^2
Y	Horizontal distance from source axis	inches
Z	Vertical distance from a virtual point source	inches

α	Thermal diffusivity	in^2/min
Δt	Terminal temperature difference between stack gas and incoming air; $t_s - t_o$	^oF
ΔT	Temperature rise above ambient air, T_o, in convection column	^oR
ϵ	Emissivity of non-black body, E/E_b	_____
ϵ_r	Emissivity, rear view of fire	_____
ϵ_s	Emissivity, side view of fire	_____
θ	Time	minutes
θ_r	Burning time of fuel particle	minutes
λ	Volume of voids per unit of fuel surface	inches
ρ_b	Apparent density of fuel bed	lbs/ft^3
ρ_g	Density of gas at constant pressure	lbs/ft^3
ρ_f	Fuel density, bone-dry	lbs/ft^3
ρ_o	Mass density of ambient air	$lbs\ sec^2/ft^4$
ρ_s	Stack gas density at constant pressure	lbs/ft^3
σ	Stefan-Boltzmann constant, 0.1714×10^{-8}	$Btu/ft^2 hr\ ^oR^4$

References

Buck, C. C., and Hughes, J. E.
1939. The solvent distillation method for determining the moisture content of forest litter. Jour. Forestry 37: 645-651.

Dunlap, Frederick
1912. The specific heat of wood. U. S. Forest Serv. Bul. 110, 27 pp.

Fons, W. L.
1946. Analysis of fire spread in light forest fuels. Jour. Agr. Res. 72: 93-121.

_____ Bruce, H. D., and Pong, W. Y.
1959. A steady-state technique for studying the properties of free-burning wood fires. In The Use of Models in Fire Research. Natl. Acad. Sci.--Natl. Res. Council Pub. 786: 219-234, illus.

_____ Bruce, H. D., Pong, W. Y., and Richards, S. S.
1960. Project fire model, summary progress report. U. S. Forest Serv. Pacific Southwest Forest Expt. Sta., 56 pp.

Gier, J. T., and Boelter, L. M. K.
1941. The silver-constantan plated thermopile. In Temperature, Its Measurement and Control in Science and Industry. 1362 pp. New York: Reinhold Publishing Corporation.

Gross, D.
1962. Experiments on the burning of cross piles of wood. Jour. of Res. of the Natl. Bur. Standards, C. Engin. and Instrumentation. 66C.

Kawagoe, K.
1958. Fire behaviour in rooms. Report of the Bldg. Res. Inst. No. 27. Japanese Ministry of Construction.

Lee, Shao-Lin, and Emmons, H. W.
1961. A study of natural convection above a line fire. Jour. Fluid Mechanics 11(3): 353-368.

MacLean, J. D.
1941. Thermal conductivity of wood. Heating, Piping, Air Conditioning 13: 380-391.

Moon, Parry
1936. Scientific Basis of Illuminating Engineering. New York: McGraw-Hill Book Co.

Scesa, S., and Sauer, F. M.
1954. Possible effects of free convection on fire behavior--laminar and turbulent line and point sources of heat. U. S. Forest Serv. Calif. Forest and Range Expt. Sta. Tech. Paper 8, 47 pp.

Spalding, D. B.
1955. Some fundamentals of combustion. In Gas Turbine Series 2. 250 pp. London: Butterworths Scientific Publications.

Thomas, P. H.
1961. Research on fires using models. The Inst. Fire Engin. Quart. XXI: 197-219.

_____ Webster, C. T., and Raftery, M. M.
1961. Some experiments on buoyant diffusion flames. Combustion and Flames 5: 359-367.

Wise, Louis E., and Jahn, Edwin C.
1952. Wood Chemistry. 2 v, 1343 pp. New York: Reinhold Publishing Corporation.

Yih, Chia-Shun
1953. Free convection due to boundary sources. In First Symposium on the Use of Models in Geophysical Fluid Dymamics. 162 pp. Supt. of Documents, U. S. Government Printing Office, Washington, D. C.

APPENDIX A

Table 4.--Experimental conditions for fires in cribs of white fir[1/] wood with lateral spacing of 1.25 inches

Fire No.	Room[2/] temp.	Fuel and fuel bed parameters								
	t_o	d_o	M_f	ρ_f	ρ_b	W_f	W_o	h_b	w_b	L_b
	°F	In	Percent	Lbs/ft^3	Lbs/ft^3	Lbs	Lbs/ft^2	In	In	In
1	67	0.453	9.8	27.1	7.29	7.54	3.31	5.44	9.25	35.5
2	70	.453	9.0	22.5	6.12	6.32	2.77	5.44	9.25	35.5
3	70	.453	10.3	31.9	8.47	8.76	3.84	5.44	9.25	35.5
4	72	.453	10.3	18.9	5.15	5.32	2.33	5.44	9.25	35.5
5	76	.453	10.4	24.5	6.58	6.81	2.99	5.44	9.25	35.5
6	73	.453	11.1	24.7	6.67	6.90	3.03	5.44	9.25	35.5
7	72	.453	11.5	24.1	6.69	2.15	1.52	2.72	5.75	35.5
8	76	.453	10.6	24.1	6.77	10.17	7.17	12.70	5.75	35.5
9	72	.453	10.8	24.1	6.32	5.74	1.43	2.72	16.25	35.5
10	75	.453	10.9	24.1	6.34	26.91	6.72	12.70	16.25	35.5
11	71	.453	10.2	24.4	6.43	11.67	2.91	5.44	16.25	35.5
12	75	.453	10.2	24.5	6.48	21.55	5.38	9.97	16.25	35.5
13	75	.453	10.1	24.3	6.60	15.93	6.99	12.70	9.25	35.5
14	77	.453	10.2	24.6	6.55	21.79	6.94	12.70	12.75	35.5
15	73	.453	10.4	29.0	7.78	10.81	3.52	5.44	9.25	47.8
16	74	.989	10.2	24.0	10.96	18.54	7.21	7.91	10.00	37.0
17	76	.454	10.6	24.1	6.41	21.37	5.33	9.99	16.25	35.5
18	74	.454	10.3	24.4	6.44	11.74	2.93	5.45	16.25	35.5
19	74	.286	10.8	24.9	4.84	7.60	3.23	8.01	9.50	35.6
20	77	.680	10.7	24.0	8.86	12.52	6.02	8.16	8.44	35.4
21	80	1.244	10.4	24.0	12.41	28.71	7.72	7.46	8.75	61.2

Table 4.--Experimental conditions for fires in cribs of white fir[1/] wood with lateral spacing of 1.25 inches (continued)

Fire No.	Room temp.[2/]	Fuel and fuel bed parameters								
	t_o	d_o	M_f	ρ_f	ρ_b	W_f	W_o	h_b	w_b	L_b
	°F	In	Percent	Lbs/ft^3	Lbs/ft^3	Lbs	Lbs/ft^2	In	In	In
22	77	0.454	10.9	24.3	6.58	9.17	2.99	5.45	9.25	47.8
23	62	.454	10.7	24.3	6.64	10.29	4.51	8.17	9.25	35.5
24	63	.989	10.7	24.0	10.94	18.53	7.21	7.91	10.00	37.0
25	66	1.244	10.6	24.1	12.46	28.82	7.74	7.46	8.75	61.2
26	60	.680	10.5	24.2	8.92	16.70	6.07	8.16	8.44	47.0
27	60	.454	10.5	24.3	6.62	9.22	3.00	5.45	9.25	47.8
28	60	.443	14.2	24.2	6.04	6.11	2.68	5.32	9.25	35.5
29	67	.443	4.8	24.3	6.06	6.13	2.69	5.32	9.25	35.5
30	57	.443	13.3	24.1	6.03	6.09	2.67	5.32	9.25	35.5
31	64	.443	4.9	24.1	6.03	6.10	2.68	5.32	9.25	35.5
32	82	.443	3.8	29.5	7.81	7.89	3.46	5.32	9.25	35.5
33	86	.443	3.8	27.1	7.15	7.24	3.18	5.32	9.25	35.5
34	85	.443	3.7	24.8	6.53	6.61	2.90	5.32	9.25	35.5
35	90	.443	3.8	20.0	5.27	5.33	2.34	5.32	9.25	35.5
36	89	.443	3.6	22.4	5.91	5.97	2.62	5.32	9.25	35.5
37	64	.443	6.1	27.0	7.12	7.19	3.15	5.32	9.25	35.5
38	66	.443	6.4	20.0	5.27	5.32	2.33	5.32	9.25	35.5
39	69	.443	6.1	24.7	6.51	6.59	2.89	5.32	9.25	35.5
40	70	.443	6.1	22.3	5.89	5.96	2.61	5.32	9.25	35.5
41	73	.443	8.6	24.6	6.48	6.55	2.87	5.32	9.25	35.5
42	75	.443	8.1	19.9	5.25	5.32	2.33	5.32	9.25	35.5
43	77	.443	8.0	29.3	7.74	7.82	3.43	5.32	9.25	35.5
44	79	.443	8.5	27.0	7.12	7.20	3.16	5.32	9.25	35.5
45	79	.443	8.0	22.4	5.91	5.97	2.62	5.32	9.25	35.5
46	71	.443	16.2	18.7	4.94	5.00	2.19	5.32	9.25	35.5
47	70	.443	16.7	24.7	6.53	6.60	2.89	5.32	9.25	35.5
48	70	.443	15.8	29.8	7.84	7.94	3.48	5.32	9.25	35.5
50	76	.443	15.6	34.1	9.00	9.11	4.00	5.32	9.25	35.5
51	76	.443	16.4	22.5	5.94	6.01	2.64	5.32	9.25	35.5
52	74	.443	14.0	20.0	5.27	5.33	2.34	5.32	9.25	35.5
53	77	.443	12.7	22.2	5.84	5.91	2.59	5.32	9.25	35.5
54	76	.443	13.4	24.5	6.46	6.53	2.86	5.32	9.25	35.5
55	74	.443	13.3	29.1	7.69	7.78	3.41	5.32	9.25	35.5
56	75	.443	13.7	27.1	7.15	7.23	3.17	5.32	9.25	35.5
57	76	.443	13.6	32.6	8.60	8.70	3.82	5.32	9.25	35.5
59	68	.443	4.8	31.6	8.35	8.44	3.70	5.32	9.25	35.5
60	74	.443	5.0	29.3	7.72	7.81	3.42	5.32	9.25	35.5
62	82	.443	4.7	24.5	6.48	6.55	2.87	5.32	9.25	35.5
63	82	.443	4.6	27.2	7.17	7.25	3.18	5.32	9.25	35.5
64	81	.443	4.7	20.0	5.29	5.34	2.34	5.32	9.25	35.5
65	84	.443	2.5	22.4	5.91	5.98	2.62	5.32	9.25	35.5

1/ White fir: (Abies concolor).
2/ Average of readings taken before and after fire.

Table 5.--Experimental conditions for fires with cribs of four different species of wood

Fire No.	Room temp.	Fuel and fuel bed parameters								
	t_o	d_o	M_f	ρ_f	ρ_b	W_f	W_o	h_b	w_b	L_b
	°F	In	Percent	Lbs/ft^3	Lbs/ft^3	Lbs	Lbs/ft^2	In	In	In
1/ 1M	65	0.454	11.3	27.8	7.50	7.77	3.41	5.45	9.25	35.5
2M	62	.454	11.4	29.4	7.95	8.24	3.61	5.45	9.25	35.5
3M	64	.454	11.3	31.9	8.62	8.93	3.92	5.45	9.25	35.5
4M	63	.454	11.4	34.2	9.24	9.57	4.20	5.45	9.25	35.5
5M	62	.454	10.9	28.3	7.64	7.91	3.47	5.45	9.25	35.5
2/ 1B	64	.454	8.3	22.5	6.03	6.25	2.74	5.45	9.25	35.5
2B	62	.454	10.6	25.4	6.81	7.06	3.10	5.45	9.25	35.5
3B	64	.454	10.6	28.3	7.59	7.85	3.44	5.45	9.25	35.5
4B	60	.454	10.6	31.0	8.31	8.61	3.78	5.45	9.25	35.5
5B	63	.454	10.0	25.4	6.82	7.07	3.10	5.45	9.25	35.5
3/ 1S	71	.456	10.6	42.9	11.63	12.10	5.31	5.47	9.25	35.5
2S	67	.456	10.4	45.2	12.25	12.73	5.58	5.47	9.25	35.5
3S	71	.456	10.5	48.1	13.05	13.57	5.95	5.47	9.25	35.5
4S	62	.456	9.8	45.2	12.25	12.74	5.59	5.47	9.25	35.5
49S	69	.456	15.5	46.3	12.32	12.80	5.61	5.47	9.25	35.5
58S	75	.456	13.2	46.7	12.41	12.89	5.65	5.47	9.25	35.5
61S	73	.456	4.6	45.4	12.08	12.55	5.50	5.47	9.25	35.5
4/ 1Y	64	.460	10.7	32.1	8.67	9.11	4.00	5.52	9.25	35.5
2Y	61	.460	10 7	35.5	9.61	10.07	4.42	5.52	9.25	35.5
3Y	68	.460	10.3	39.2	10.59	11.12	4.88	5.52	9.25	35.5
4Y	66	.460	10.8	41.4	11.18	11.73	5.14	5.52	9.25	35.5
5Y	68	.460	10.4	46.9	12.67	13.29	5.83	5.52	9.25	35.5

1/ Magnolia, (~~Abies concolor~~), 2/ basswood (Tilia americana), 3/ sugar maple (Acer saccharum), 4/ longleaf pine (Pinus palustris).

Table 6.--Experimental results for fires in cribs of white fir wood

Fire No.	Burning parameters			Flame dimensions		Heat rates		Stack[1/] gas conditions			
	θ_r	G	R	D	L	Q	Q_c	$\bar{U}$	Δt	t_s	ρ_s
	Min	Lbs/ft^{2}min	In/min	In	In	Btu/sec	Btu/sec	Ft/sec	°F	°F	Lbs/ft^3
1	2.8	1.17	1.51	4.2	33.0	42.9	-	-	-	-	-
2	2.4	1.17	1.91	4.5	35.3	45.8	-	-	-	-	-
3	3.6	1.06	1.23	4.4	33.6	40.7	-	-	-	-	-
4	1.8	1.25	2.38	4.4	36.9	47.8	-	-	-	-	-
5	2.8	1.07	1.74	4.8	35.4	44.7	-	-	-	-	-
6	2.6	1.14	1.79	4.7	34.8	46.6	-	-	-	-	-
7	2.7	.56	1.41	3.8	17.2	11.4	-	-	-	-	-
8	3.7	1.92	1.68	6.2	42.8	64.5	-	-	-	-	-
9	3.0	.46	1.38	4.2	18.9	29.9	-	-	-	-	-
10	3.8	1.77	1.92	7.2	66.8	195.4	-	-	-	-	-
11	2.7	1.12	1.87	5.1	38.0	87.5	-	-	-	-	-
12	3.2	1.66	1.75	5.6	52.8	142.5	-	-	-	-	-
13	3.2	2.19	1.87	5.9	56.5	112.5	-	-	-	-	-
14	3.2	2.14	1.86	6.0	64.1	156.0	-	-	-	-	-
15	2.6	-	1.37	3.6	33.8	-	-	-	-	-	-
16	8.5	.83	1.15	9.8	39.5	77.0	-	-	-	-	-
17	3.2	1.62	1.78	5.8	53.0	143.8	-	-	-	-	-
18	3.0	.97	1.61	4.8	38.3	71.4	-	-	-	-	-
19	2.0	1.61	2.13	4.2	45.1	61.0	-	-	-	-	-
20	5.4	1.10	1.24	6.7	39.4	58.6	-	-	-	-	-
21	11.0	.68	1.25	13.8	29.2	78.2	-	-	-	-	-

Table 6.--Experimental results for fires in cribs of white fir wood (continued)

Fire	Burning parameters			Flame dimensions		Heat rates		Stack[1/] gas conditions			
No.	θ_r	G	R	D	L	Q	Q_c	$\bar{U}$	Δt	t_s	ρ_s
	Min	Lbs/ft^{2}min	In/min	In	In	Btu/sec	Btu/sec	Ft/sec	^oF	^oF	Lbs/ft^3
22	3.0	0.99	1.78	5.3	37.2	45.8	-	-	-	-	-
23	2.9	1.52	1.81	5.3	41.3	70.3	-	-	-	-	-
24	7.5	.94	1.30	9.8	34.6	87.0	-	-	-	-	-
25	12.2	.62	1.10	13.5	27.0	69.3	-	-	-	-	-
26	5.2	1.15	1.38	7.2	38.3	65.6	-	-	-	-	-
27	3.1	.96	1.74	5.4	33.5	45.1	-	-	-	-	-
28	-	-	1.71	-	-	39.4	-	-	-	-	-
29	-	-	2.67	-	-	61.8	-	-	-	-	-
30	-	-	1.68	-	-	38.6	-	-	-	-	-
31	2.0	1.34	2.54	5.0	33.6	58.4	22.8	25.3	16.2	78	0.0738
32	2.7	1.28	2.03	5.4	37.9	60.1	32.7	26.6	23.1	102	.0707
33	2.4	1.29	2.19	5.3	39.6	59.3	33.1	27.8	22.6	107	.0700
34	2.1	1.37	2.44	5.1	40.9	60.6	33.9	27.1	23.6	105	.0703
35	2.5	.92	4.29	10.8	44.7	86.1	49.7	27.8	34.9	124	.0680
36	-	-	3.23	-	-	72.3	38.0	27.1	26.9	115	.0691
37	2.5	1.26	1.94	4.8	32.4	52.7	24.0	25.3	17.1	79	.0737
38	2.2	1.06	3.11	6.7	36.4	62.1	28.5	25.5	20.4	85	.0728
39	2.5	1.14	2.06	5.1	35.0	50.8	25.1	25.5	18.0	86	.0727
40	2.1	1.24	2.42	5.0	34.7	54.1	25.4	25.5	18.2	87	.0725
41	2.5	1.14	1.85	4.6	31.9	46.0	20.5	25.5	14.7	87	.0725
42	1.8	1.24	2.66	4.9	34.6	53.2	25.3	25.2	18.5	91	.0721
43	-	-	1.50	-	-	44.0	21.8	25.6	15.7	91	.0721
44	2.6	1.16	1.70	4.5	32.6	46.0	22.5	25.7	16.2	93	.0718
45	2.2	1.14	2.31	5.2	34.5	52.0	25.3	25.7	18.3	97	.0713
46	2.4	.88	1.80	4.4	26.7	33.8	13.9	25.4	9.9	81	.0734
47	3.7	.76	1.22	4.5	25.4	30.2	12.1	25.4	8.6	80	.0735
48	4.6	.73	1.02	4.7	24.0	30.3	13.6	25.3	9.7	79	.0737
50	4.5	.87	.96	4.3	24.4	32.8	14.2	26.1	9.9	85	.0728
51	3.0	.87	1.34	4.0	25.5	30.4	12.4	25.5	8.9	85	.0728
52	2.5	.91	1.84	4.6	27.8	36.8	13.9	21.9	11.6	86	.0727
53	2.7	.95	1.68	4.5	28.3	37.4	14.4	21.0	12.6	87	.0725
54	2.9	.96	1.54	4.5	27.0	37.8	16.2	20.6	14.4	89	.0723
55	3.8	.87	1.20	4.6	26.5	35.1	14.4	21.0	12.6	87	.0725
56	3.2	.94	1.26	4.1	24.8	34.0	12.0	19.4	11.3	84	.0730
57	3.8	.98	1.08	4.1	27.8	35.4	12.5	19.4	11.8	86	.0727
59	2.9	1.25	1.88	5.4	30.8	59.1	19.7	27.2	13.1	81	.0734
60	2.9	1.16	2.23	6.4	33.9	65.2	26.1	23.9	20.2	93	.0718
62	2.1	1.34	2.46	5.1	43.8	60.2	26.4	24.4	20.2	99	.0710
63	2.2	1.38	2.20	4.9	39.7	59.3	23.4	24.0	18.2	99	.0710
64	2.0	1.13	3.42	6.9	42.8	68.4	33.2	27.2	23.0	104	.0704
65	2.1	1.19	3.17	6.8	37.3	71.0	32.8	25.0	24.9	107	.0700

1/ Stack area was 3.14 ft^2 for fires 31 through 65.

Table 7.--Experimental results for fires in cribs of four different species of wood

Fire	Burning parameters			Flame dimensions		Heat rates		Stack[1/] gas conditions			
No.	θ_r	G	R	D	L	Q	Q_c	$\bar{U}$	Δt	t_s	ρ_s
	Min	Lbs/ft^{2}min	In/min	In	In	Btu/sec	Btu/sec	Ft/sec	^oF	^oF	Lbs/ft^3
1M	2.7	1.25	1.53	4.1	31.9	44.3	25.5	31.9	17.2	81	0.0734
2M	3.2	1.13	1.49	4.7	30.3	45.7	26.0	33.5	16.6	79	.0737
3M	3.2	1.21	1.35	4.3	29.1	44.9	24.4	31.9	16.4	80	.0735
4M	3.3	1.25	1.15	3.8	30.7	41.0	23.4	31.8	15.7	77	.0740
5M	3.1	1.11	1.56	4.8	33.4	46.0	28.3	30.6	19.9	80	.0735
1B	-	-	2.64	-	-	59.6	-	-	-	-	-
2B	2.1	1.45	2.02	4.2	33.2	51.3	29.0	31.9	19.5	79	.0737
3B	2.5	1.32	1.85	4.7	33.2	52.0	29.0	31.9	19.6	82	.0732
4B	2.9	1.24	1.63	4.8	32.7	50.1	27.6	-	-	-	-
5B	2.3	1.29	2.05	4.8	35.1	52.1	31.8	30.5	22.5	82	.0732
1S	4.2	1.21	.88	3.7	26.1	38.5	18.0	32.3	12.2	91	.0721
2S	3.9	1.36	.82	3.2	26.6	37.4	20.2	31.4	13.8	79	.0737
3S	4.7	1.15	.74	3.5	25.2	34.7	16.3	31.5	11.2	85	.0728
4S	3.8	1.39	.86	3.3	26.1	39.5	18.9	30.5	13.1	72	.0747
49S	5.9	.88	.66	3.9	20.8	29.7	11.6	25.3	8.2	77	.0740
58S	5.9	.89	.74	4.4	23.8	33.6	10.5	20.5	9.3	82	.0732
61S	4.3	1.26	1.24	5.3	30.6	57.8	17.5	24.1	13.2	84	.0730
1Y	4.2	.91	1.08	4.6	26.3	37.2	18.8	30.0	13.3	75	.0742
2Y	3.5	1.22	.93	3.3	26.8	35.5	18.4	30.8	12.6	71	.0748
3Y	3.9	1.21	.87	3.4	26.7	36.4	18.8	30.2	13.4	82	.0732
4Y	4.5	1.12	.76	3.4	25.6	33.6	17.2	29.6	12.5	80	.0735
5Y	4.9	1.14	.67	3.3	26.2	33.4	15.8	29.7	11.4	79	.0737

1/ Stack area was 2.64 ft^2 for all fires except 49S, 58S, and 61S, where the area was 3.14 ft^2.

Table 8.--Irradiance[1/] for fires with cribs of white fir wood

Fire No.	Irradiance (I)		
	Front	Rear	Side
	Btu/ft^{2}hr	Btu/ft^{2}hr	Btu/ft^{2}hr
31	9.2	17.6	17.4
32	10.3	16.2	18.1
33	9.8	15.3	16.5
34	9.8	15.5	16.7
35	15.0	20.5	23.6
36	11.8	18.0	20.3
37	9.5	15.5	15.8
38	11.3	16.9	17.0
39	9.7	15.3	16.0
40	9.7	16.0	16.5
41	9.7	13.7	14.1
42	9.5	15.0	16.2
43	8.2	13.2	13.9
44	8.0	13.2	14.8
45	9.3	14.4	15.3
46	4.7	11.2	9.7
47	4.3	10.0	9.2
48	4.2	10.0	9.4
49	3.3	7.3	8.0
50	3.8	10.0	9.9
51	4.0	9.4	8.5
52	5.8	11.9	9.7
53	6.3	12.3	10.1
54	6.5	12.5	9.9
55	5.5	11.4	9.7
56	4.8	10.3	7.8
57	5.0	11.4	9.0
58	5.0	9.4	7.8
59	11.7	18.6	16.0
60	11.3	17.8	14.6
61	9.0	13.2	11.5
62	11.3	17.3	16.5
63	11.5	18.2	16.9
64	12.6	18.7	18.1
65	13.2	19.6	22.6

1/ For radiometer positions see figure 11.

Table 9.--Irradiance[1/] for fires in cribs of magnolia, basswood, sugar maple, and southern yellow pine

Fire No.	Irradiance (I)		
	Front	Rear	Side
	Btu/ft^{2}hr	Btu/ft^{2}hr	Btu/ft^{2}hr
1M	6.2	13.5	11.0
2M	...	14.4	12.6
3M	7.2	...	12.3
4M	7.2	13.5	10.7
5M	7.0	14.4	13.2
1B	...	...	...
2B	8.2	14.8	13.2
3B	7.7	13.7	13.2
4B	7.2	14.3	12.6
5B	8.3	14.0	14.8
1S	...	...	...
2S	...	...	...
3S	4.1	9.5	7.7
4S	6.0	12.5	7.7
49S	3.3	7.3	8.0
58S	5.0	9.4	7.8
61S	9.0	13.2	11.5
1Y	5.6	12.5	7.9
2Y	5.6	12.5	8.1
3Y	5.9	12.3	8.1
4Y	5.3	11.3	7.0
5Y	4.8	10.9	6.8

1/ For radiometer positions see figure 11.

APPENDIX B

The radiant energy exchange between surfaces depends on the emissive, absorptive, and reflective properties of the surface and also on their geometrical shapes and arrangement. The ratio of the irradiance at a point and the unit energy emitted from a surface is defined as the geometrical view factor between the surface and the point. The shape of the flaming zone of a crib fire is approximately rectangular when viewed from the side, front, or rear. The positions at which radiometers were placed to measure irradiance for the flaming zone of a crib fire are shown in figure 11. The radiometers are aimed at a point 2-1/2 feet above the base of the crib and on the vertical axis of the flaming zone. In determining the view factor between a rectangular source and a given point, it is convenient to divide the surface of the source into several smaller rectangular areas (Moon, 1936). The view factor for the total surface is then equal to the sum of the view factors for the smaller areas. Thus the surface of the flaming zone for a crib fire may be divided into four rectangular areas, each having one corner at the aiming point of the radiometer viewing that surface.

Consider a point, P, that lies on a perpendicular erected at one corner of a rectangular source with constant emissive power (fig. 14). If the point lies in a plane parallel to the source, the equation for the view factor of the rectangular source (Moon, 1936) is

$$F_z = \frac{1}{2\pi}\left[\frac{z}{\sqrt{x^2 + z^2}} \sin^{-1}\frac{y}{r} + \frac{y}{\sqrt{x^2 + y^2}} \sin^{-1}\frac{z}{r}\right] \qquad (21)$$

where $r = (x^2 + y^2 + z^2)^{\frac{1}{2}}$.

The corresponding equation for the view factor referring to a point in a plane perpendicular to the rectangular source (Moon, 1936) is

$$F_y = \frac{1}{2\pi}\left[\tan^{-1}\frac{y}{x} - \frac{x}{\sqrt{x^2 \quad z^2}} \sin^{-1}\frac{y}{r}\right] \qquad (22)$$

View factors, F_z and F_y, calculated by equations (21) and (22) for a range of values z/x and y/x, are presented in tables 10 and 11, respectively. These tables cover the range of view factors applicable to laboratory crib fires. Tables of view factors for larger rectangular sources, with y and z extending to infinity, are given by Moon (1936).

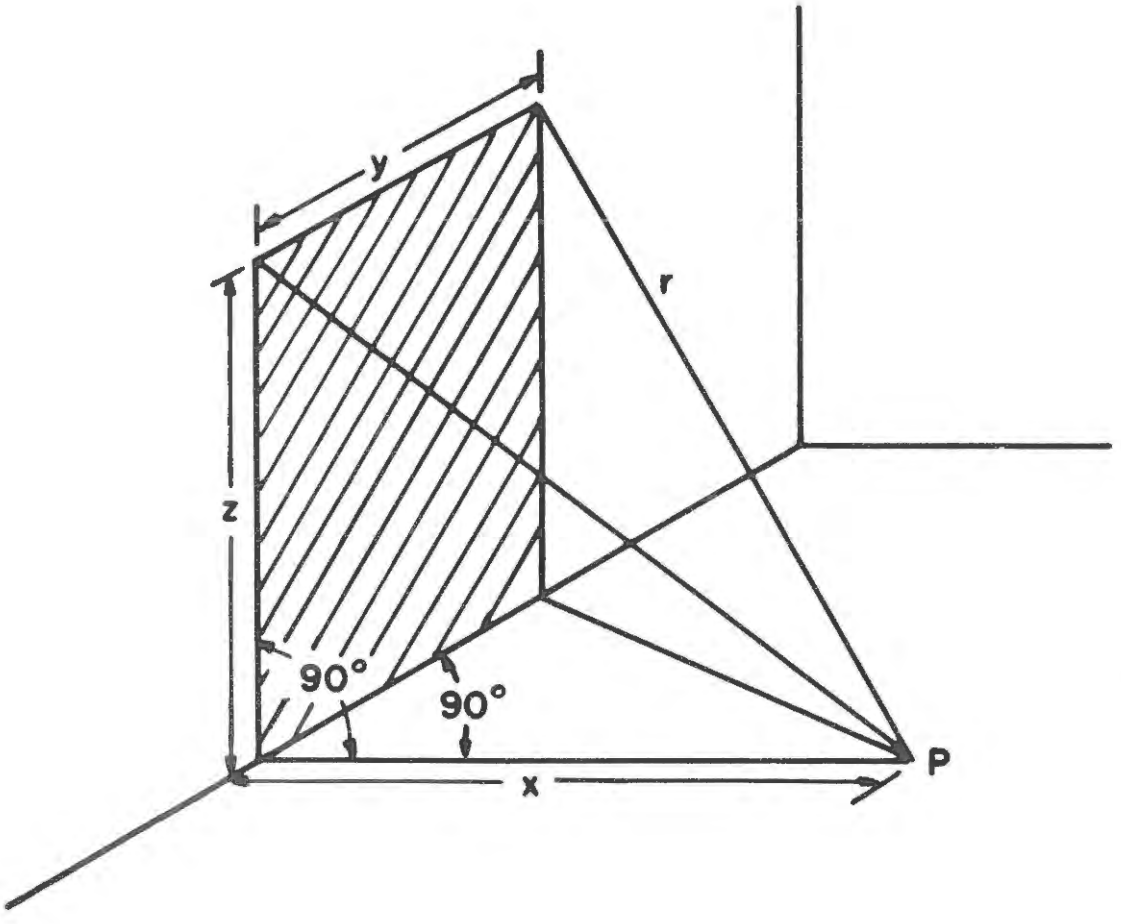

Figure 14. --Projected view of a rectangular source, with reference to a point, P.

Table 10.--View factors, $F_z \times 10^4$, with reference to a parallel plane

(calculated by equation (21))

z/x	y/x									
	0.01	0.02	0.03	0.04	0.05	0.06	0.07	0.08	0.09	0.10
0.05	1.54	3.10	4.70	6.20	7.72	9.38	10.9	12.5	14.0	15.6
.06	1.84	3.72	5.64	7.44	9.26	11.3	13.1	15.0	16.9	18.7
.07	2.15	4.34	6.58	8.68	10.8	13.1	15.3	17.5	19.7	21.8
.08	2.46	4.96	7.52	9.92	12.3	15.0	17.4	20.0	22.5	24.9
.09	2.76	5.58	8.46	11.2	13.9	16.9	19.6	22.5	25.3	28.0
.10	3.07	6.20	9.40	12.4	15.4	18.8	21.8	25.0	28.1	31.1
.11	3.38	6.82	10.3	13.6	17.0	20.6	24.0	27.5	30.9	34.2
.12	3.68	7.44	11.3	14.9	18.5	22.5	26.2	30.0	33.7	37.3
.13	3.99	8.06	12.2	16.1	20.1	24.4	28.3	32.5	36.5	40.4
.14	4.30	8.68	13.2	17.4	21.6	26.3	30.5	35.0	39.3	43.5
.15	4.60	9.30	14.1	18.6	23.1	28.2	32.7	37.5	42.2	46.6
.16	4.91	9.92	15.0	19.8	24.7	30.0	34.9	40.0	45.0	49.8
.17	5.22	10.5	16.0	21.1	26.2	31.9	37.1	42.5	47.8	52.9
.18	5.53	11.2	16.9	22.3	27.8	33.8	39.2	45.0	50.6	56.0
.19	5.83	11.8	17.9	23.6	29.3	35.7	41.4	47.5	53.4	59.1
.20	6.14	12.4	18.8	24.8	30.9	37.5	43.6	50.0	56.2	62.2

Table 11.--View factors, $F_y \times 10^5$, with reference to a perpendicular plane

(calculated by equation (22))

z/x	y/z									
	0.01	0.02	0.03	0.04	0.05	0.06	0.07	0.08	0.09	0.10
0.05	0.400	0.80	1.20	1.60	2.00	2.40	2.80	3.20	3.60	4.00
.06	.582	1.16	1.75	2.33	2.91	3.49	4.07	4.66	5.24	5.82
.07	.774	1.55	2.32	3.10	3.87	4.64	5.42	6.19	6.97	7.74
.08	1.01	2.03	3.04	4.05	5.06	6.08	7.09	8.10	9.12	10.1
.09	1.26	2.52	3.78	5.04	6.30	7.57	8.83	10.1	11.4	12.6
.10	1.56	3.12	4.68	6.24	7.80	9.36	10.9	12.5	14.0	15.6
.11	1.88	3.75	5.63	7.50	9.38	11.3	13.1	15.0	16.9	18.8
.12	2.22	4.44	6.66	8.88	11.1	13.3	15.5	17.8	20.0	22.2
.13	2.63	5.26	7.88	10.5	13.1	15.8	18.4	21.0	23.6	26.3
.14	3.07	6.13	9.20	12.3	15.3	18.4	21.5	24.5	27.6	30.7
.15	3.51	7.03	10.5	14.1	17.6	21.1	24.6	28.1	31.6	35.1
.16	4.00	8.00	12.0	16.0	20.0	24.0	28.0	32.0	36.0	40.0
.17	4.46	8.93	13.4	17.9	22.3	26.8	31.2	35.7	40.2	44.6
.18	4.97	9.93	14.9	19.9	24.8	29.8	34.8	39.7	44.7	49.7
.19	5.52	11.0	16.6	22.1	27.6	33.1	38.6	44.2	49.7	55.2
.20	6.08	12.2	18.3	24.3	30.4	36.5	42.6	48.7	54.8	60.9

DISTRIBUTION LIST

	No. of copies
Wright Air Development Div. WCLEMH Wright-Patterson AFB, Ohio	1
Federal Fire Council 4316 General Services Bldg. Washington 25, D. C.	2
National Research Council National Academy of Sciences Committee on Fire Research Washington 25, D. C.	2
U. S. Dept. of the Interior Bureau of Mines Branch of Explosives Research Washington 25, D. C.	2
National Science Foundation Director for Mathematical, Physical & Engng Sciences Washington 25, D. C.	1
Office of Civil Defense The Pentagon Washington 25, D. C.	6
Prof. H. C. Hottel Director, Fuels Res. Lab. Mass. Institute of Technol. Cambridge 39, Massachusetts	1
Dr. William H. Avery Res. & Dev. Supervisor Applied Physics Laboratory The Johns Hopkins University 8621 Georgia Avenue Silver Spring, Maryland	1
Mr. Horatio Bond National Fire Protection Assn 60 Batterymarch Street Boston 10, Mass.	1
Mr. A. A. Brown, Director Div. of Forest Fire Research U. S. Forest Service Dept. of Agriculture Washington 25, D. C.	6
Dr. Howard W. Emmons Dept. of Mechanical Engineering Harvard University Cambridge 38, Massachusetts	1
Mr. Joseph Grumer U. S. Bureau of Mines 4800 Forbes Avenue Pittsburgh 13, Pennsylvania	1
Mr. J. B. Macauley, Deputy Director Defense Res. & Engineering Department of Defense Washington 25, D. C.	1
Dr. Walter T. Olson Lewis Research Center Natl Aeronaut. & Space Admin. 21000 Brookpark Road Cleveland, Ohio	1
Dr. A. F. Robertson, Chief Fire Research Section National Bureau of Standards Washington 25, D. C.	50
Dr. Walter G. Berl Applied Physics Laboratory 8621 Georgia Avenue Silver Spring, Maryland	1
Mr. B. P. Botteri Wright Air Development Div. WWRMFE-3 Wright-Patterson AFB, Ohio	1

	No. of copies
Chief, Bureau of Ships Department of the Navy Washington 25, D. C. Attn: Code 340	2
Director, Naval Res. Lab. Washington 25, D. C. Attn: Tech. Information Off.	2
Naval Radiological Def. Lab. San Francisco 24, California Attn: Technical Library	1
Technical Director Res. & Engng Division Office of Quartermaster General Department of the Army Washington 25, D. C.	1
Research Director Chemical & Plastics Division Quartermaster Res. & Engng Comm. Natick, Massachusetts	1
AF Office of Sci. Res. (SRLT) Washington 25, D. C.	1
Commanding Officer Diamond Ordnance Fuze Labs. Washington 25, D. C. Attn: Tech. Reference Section (ORDTL 06.33)	1
U. S. Naval Civil Eng. Res. & Evaluation Lab. Div. Research Port Hueneme, California	1
U. S. Bureau of Mines 4800 Forbes Street Pittsburgh 13, Pennsylvania Attn: Dr. R. W. Van Dolah	1
U. S. National Bureau of Standards Office of Technical Information Washington 25, D. C.	1
Chief Fire Supression Section Special Equipment Branch Engr. Res. & Devel. Laboratory Fort Belvior, Virginia Attn: Mr. J. E. Malcolm	1
Director Advanced Research Projects Agency The Pentagon Washington 25, D. C. Attn: Mr. W. W. Bolton, Jr.	4
Dr. Mathew H. Braidech Natl Board of Fire Underwriters 85 John Street New York 38, New York	1
Mr. Clarence F. Castle Properties and Installation Office Asst Secy of Defense Washington, D. C.	1
Dr. Bernard Lewis Combustion & Explosives Res. 1007 Oliver Building Pittsburgh 22, Pennsylvania	1
Mr. Norman J. Thompson Millers Mill Road Dover, Massachusetts	1
Dr. Richard Tuve Chemistry Division U. S. Naval Res. Laboratory Washington, D. C.	1

	No. of copies
Office of Director of Defense Research and Engineering The Pentagon Washington 25, D. C. Attn: Mr. Willis B. Foster	2
Southwest Research Institute 8500 Culebra Road San Antonio, Texas Attn: Dr. W. D. Weatherford	1
Dept. Mechanical Engineering Inst. of Technology Univ. of Minnesota Minneapolis 14, Minnesota Attn: Prof. Perry L. Blackshear,Jr.	1
Battelle Memorial Institute 505 King Avenue Columbus 1, Ohio Attn: Mr. A. A. Putman	1
U. S. Forest Service Southern Forest Fire Lab. P. O. Box 1421, Macon, Ga. Attn: K. W. McNasser	1